Program

- Accelerators and detectors
- QCD Measurements
- b and c quark properties
- top properties
- new physics searches

Colliders and Detectors

Contents

Why Colliders

Particles with high mass and low production cross section had/have to be experimentally discovered to verify the validity of the Standard Model

Colliders have been and are a very powerful tool.

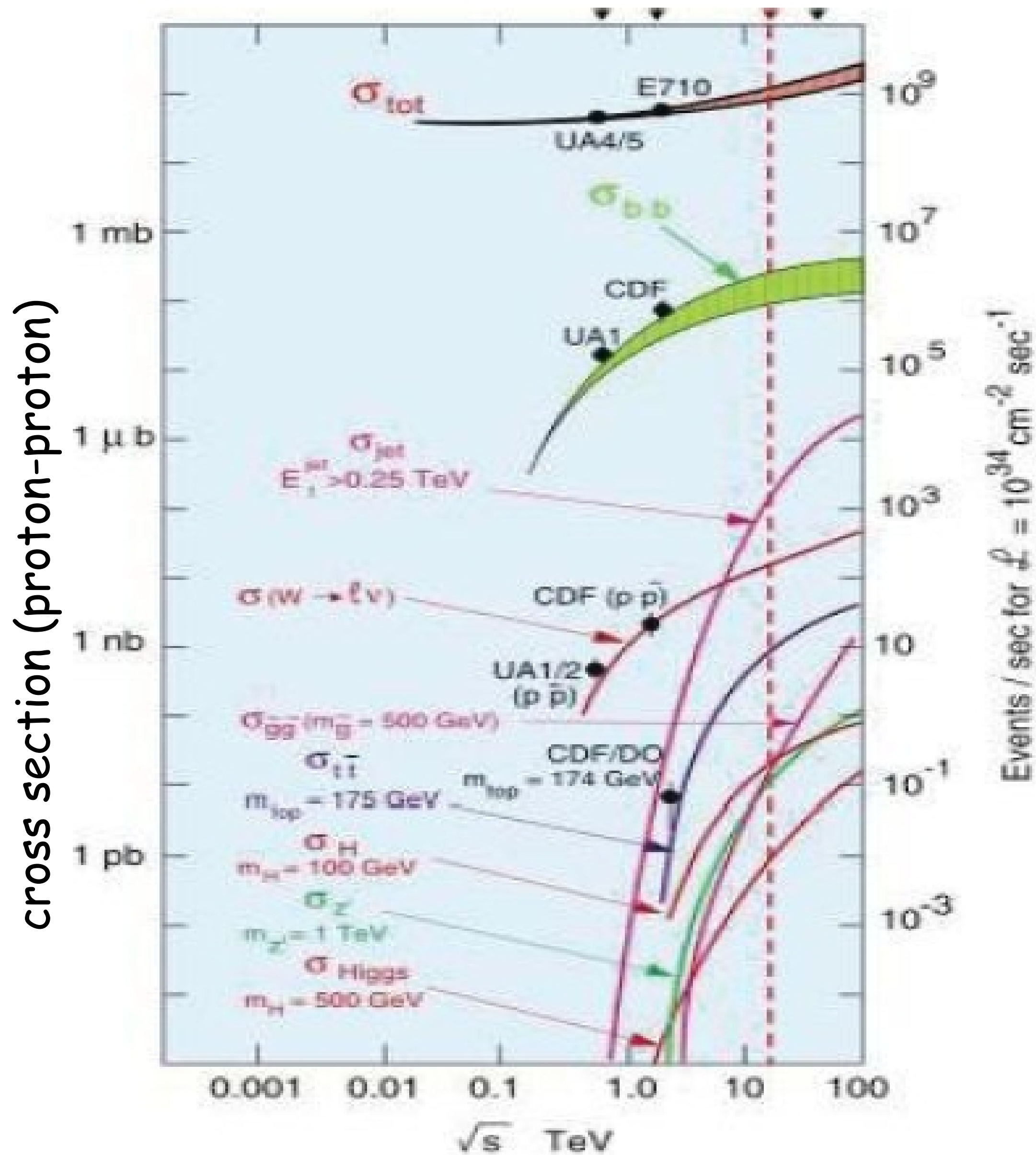

Colliders vs. fixed target: Rate

Fixed target:

Beam with n_1 particles per second

Target of length l with density particles n_2 per m^3

For each single particle the number of interaction in the target:

$$N = \sigma_{int} \cdot n_2 \cdot l$$

where σ_{in} is the interaction cross section.

If the target is larger than the beam, the rate R

$$R = dN/dt = \sigma_{int} \cdot n_1 \cdot n_2 \cdot l$$

$$R = \sigma_{int} \cdot L$$

$L = n_1 \cdot n_2 \cdot l$ is the luminosity $[cm^{-2}s^{-1}]$

The luminosity depends only on target and beam

Colliders vs. fixed target: Rate (2)

Colliders

Two beams with n_1 and n_2 particles per area

$$\frac{dn_1}{ds}=\frac{n_1}{2\pi\sigma_x\sigma_y}e^{-\left(x^2/2\sigma_x^2+y^2/2\sigma_y^2\right)}$$

$$\frac{dn_2}{ds}=\frac{n_2}{2\pi\sigma_x\sigma_y}e^{-\left(x^2/2\sigma_x^2+y^2/2\sigma_y^2\right)}$$

Gaussian distribution normalized to number of particles

Number of particles n_1 in an area dxdy $dn_1(x,y)=\frac{n_1}{2\pi\sigma_x\sigma_y}e^{-\left(x^2/2\sigma_x^2+y^2/2\sigma_y^2\right)}\cdot dxdy$

The probability of interaction of a particle in beam 1 in (x,y) is the number of particles of beam 2 in the area σ_{in}

$$p(x,y)=\mathrm{dn}_2(x,y)=\frac{n_2}{2\pi\sigma_x\sigma_y}e^{-\left(x^2/2\sigma_x^2+y^2/2\sigma_y^2\right)}\cdot\sigma_{\mathrm{int}}$$

Colliders vs. Fixed Target: Rate(3)

Total number of interaction per bunch per crossing N_{int}:

$$N_{\text{int}} = \int dn_1(x,y)\,p(x,y) = \sigma_{int}\frac{n_1 n_2}{4\pi^2\sigma_x^2\sigma_y^2}\int e^{-\left(\frac{x^2}{\sigma_x^2}+\frac{y^2}{\sigma_y^2}\right)}dxdy$$

$$= \sigma_{int}\frac{n_1 n_2}{4\pi^2\sigma_x^2\sigma_y^2}\int_{-\infty}^{+\infty} dx\cdot e^{-x^2\sigma_x^2}\int_{-\infty}^{+\infty} dy\cdot e^{-y^2\sigma_y^2} = \sigma_{int}\frac{n_1 n_2}{4\pi\sigma_x\sigma_y}$$

$$\int_{-\infty}^{+\infty} dx e^{-\frac{x^2}{\sigma_x^2}} = \sqrt{\pi}\,\sigma\frac{1}{\sqrt{2\pi}\,\sigma\sqrt{2}}\int dx e^{-\frac{x^2}{2(\sigma\sqrt{2})^2}} = \sqrt{\pi}\cdot\sigma$$

Given k packets in each bunch with a frequency f, the rate R

$$R = N_{\text{int}}\cdot \text{f/k} = \sigma_{\text{int}}\cdot L = \frac{n_1 n_2}{4\pi\sigma_x\sigma_y k}\cdot f\sigma_{int}$$

$$\Rightarrow \qquad L = \frac{n_1 n_2 f}{4\pi\sigma_x\sigma_y k}$$

Colliders vs. Fixed Target: Rate

Assumptions:

- same C.M. Energy
- same interaction cross section (e.g. $\sigma_{in} \sim 1\mu b = 1 \cdot 10^{-24}\ cm^2$)

Fixed target

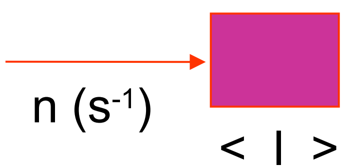

n_1= incident beam density =10^{12} particles s^{-1}

ρ= target density = 1gr/cm^3

l= target thickeness =1cm

σ_{int}= 1μb

A= Avogadro number = 6×10^{23}

$$R = n_1 \cdot n_2 \cdot l \cdot \sigma_i = n_1 \cdot \rho \cdot l \cdot A \cdot \sigma_i = 6 \times 10^5\, s^{-1}$$

Colliders vs. Fixed Target: Rate cont'd

Collider

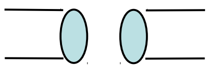

$n_1=n_2=$ beam particles

$i_1= i_2=50$ mA ➔ $n_1=n_2=i_{1,2}/ef = 50 \cdot 10^{-3} / (1.6 \cdot 10^{-19} \cdot 10^{6}) = 3.1 \times 10^{11}$

F= transverse section of beams= 0.1×0.01 cm^2

B= bunch number= 1

f= revolution frequency = 10^6 s^{-1}

$$R = \frac{n_1 \cdot n_2 \cdot f}{F} \cdot \sigma_{\text{int}} = \frac{i_1 \cdot i_2}{f \cdot e^2 \cdot F} \cdot \sigma_{\text{int}} \cong 100 s^{-1}$$

Center of Mass Energy

Beam/target particles interaction:

Fixed target

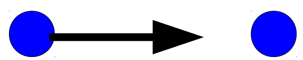

E_1, P_1 E_2, P_2

$P_2 = 0$ in the lab. system

$$E_{CM}^2 = m_1^2 + m_2^2 + 2E_1 \cdot m_1$$

Collider

E_1, P_1 E_2, P_2

Collinear beams:

$$E_{CM}^2 = m_1^2 + m_2^2 + 4E_1 E_2$$

Center of Mass Energy cont'd

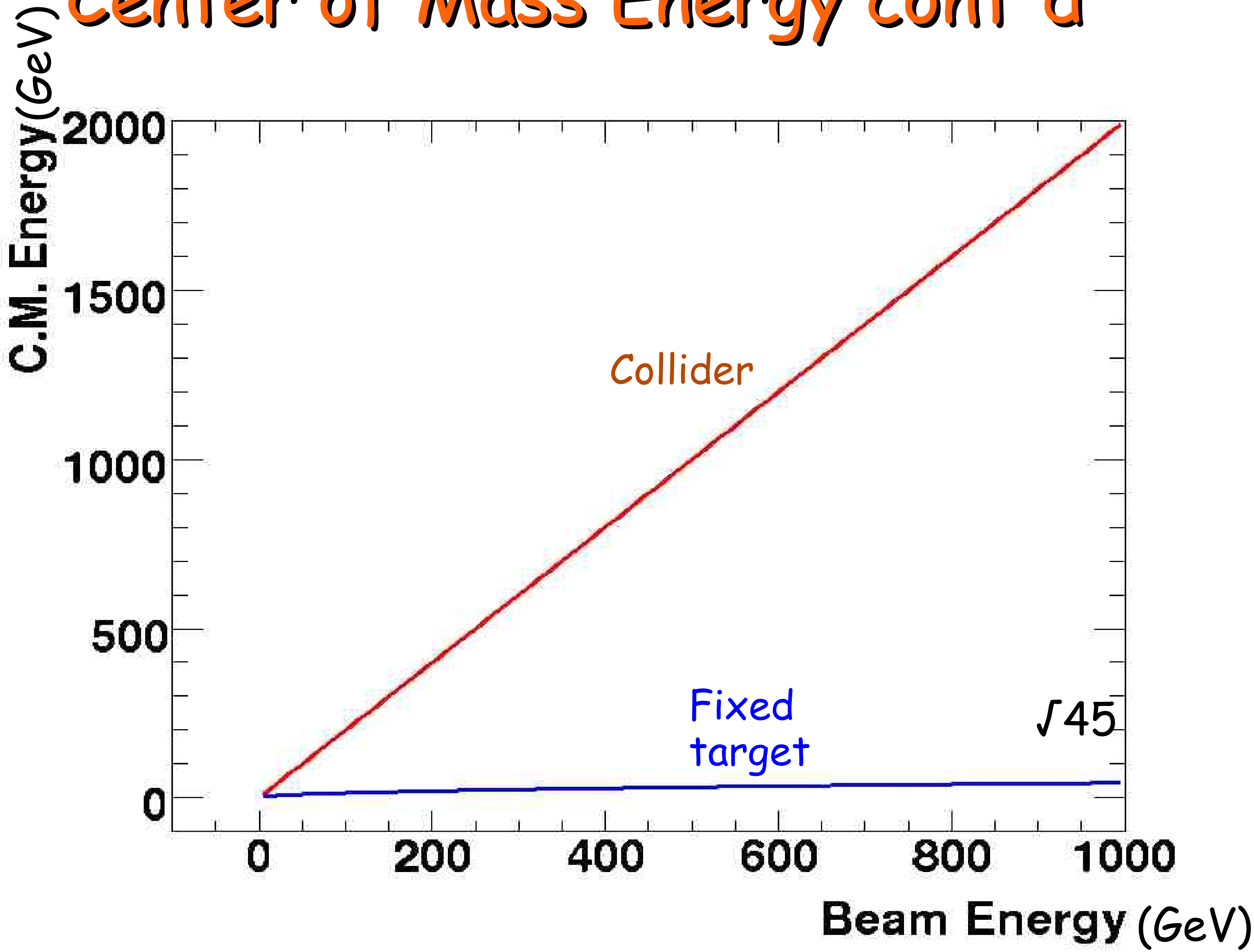

Luminosity

$$L=\frac{n_1 n_2 f B}{4\pi\sigma_x\sigma_y}=\frac{N^2 f B}{A}$$

$n_1=n_2=N$, B=number of bunches

A= interaction area

Luminosity determination

- crossing angle:
  often used to avoid unwanted collisions in machines with many bunches like LHC that has ~3000 closely spaced bunches. At LHC the crossi angle is ~ 300 μrad. at ISR it was 18°

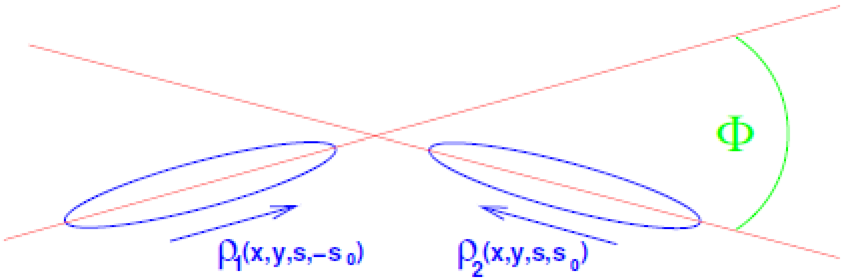

- transverse offset:
  beams do not collide head-on, but with a small transverse offset

Luminosity - 2

$$\sigma = \sqrt{\beta(s) \cdot \epsilon}$$

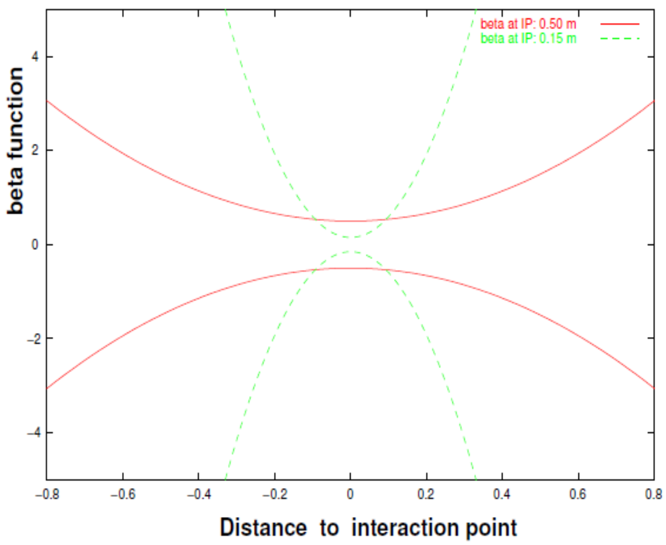

- hourglass effect
  in the basic model, beam particle densities are assumed uncorrelated in the transverse and longitudinal plane with the transverse beam size constant. In the real machine the beam size is minimal at the interaction point and increases with the distance.
- non-Gaussian beam profiles

Integrated luminosity:

$$L_i = \int_0^T L(t)\,dt$$

T=sensitive time, ie no dead time

Realistic model of the luminosity as function of time $L(t) = L_0 e^{-\frac{t}{\tau}}$

Optimization of Integrated Luminosity

In a data taking the goal is to optimize the integrated luminosity.

Two phases:

- preparation phase with a time, t_p
- run period, t_r , free parameter; users decide how long the run is

assuming $L(t) = L_0 e^{-\frac{t}{\tau}}$ ‹L(t)› has to be maximized

$$<\mathcal{L}> = \frac{\int_0^{t_r} \mathcal{L}(t)dt}{t_r + t_p} = \mathcal{L}_0 \cdot \tau \cdot \frac{1 - e^{-t_r/\tau}}{t_r + t_p}$$

it can be solved to obtain $t_r \approx \tau \cdot \ln(1 + \sqrt{2t_p/\tau} + t_p/\tau)$

Assuming LHC parameters t_p ~10h, τ~15h → t_r ~ 15h

A bit of History

1961 AdA, Frascati Italy
1964 VEPP 2 Novosibirsk, URSS
1965 ACO, Orsay, France
1969 ADONE, Frascati
1970 ISR, CERN Swiss
1971 CEA, Cambridge, USA
1972 SPEAR Stanford USA 8 GeV
1974 DORIS, Amburg, Germany
1975 VEPP-2M Novosibirsk, URSS
1978 PETRA Amburgo Germany 45 GeV
1979 CESR Cornell USA
1980 PEP Stanford USA
1981 Sp-parS CERN Swiss 630 GeV
1982 TEVATRON Fermilab USA 2TeV
1989 SLC, Stanford USA 90 GeV
1989 BEPC, Bejin china

1989 LEP CERN 205 GeV
1992 HERA, Amburg Germany
1994 VEPP-4M Novosibirsk Russia
1998 PEP-II Stanford USA
1999 DAΦNE, Frascati Italy
1999 KEKB Tsukuba Japan
2003 VEPP-2000 Novosibirsk Russia
2008 LHC CERN Swiss 14 TeV

electron-positron
proton-proton
electron-proton
proton-antiproton

Hadron Colliders

ISR: p-p and first p-pbar $\sqrt{s}$= 63 GeV (1970-1980) (DC)
SpS: p-pbar $\sqrt{s}$= 630 GeV (1980-1991)
Tevatron: p-pbar $\sqrt{s}$= 1.960 TeV (1978-2011)
LHC: p-p $\sqrt{s}$= 14 TeV (1998-)

ISR(Intersecting Storage Rings)

1971: first p-p

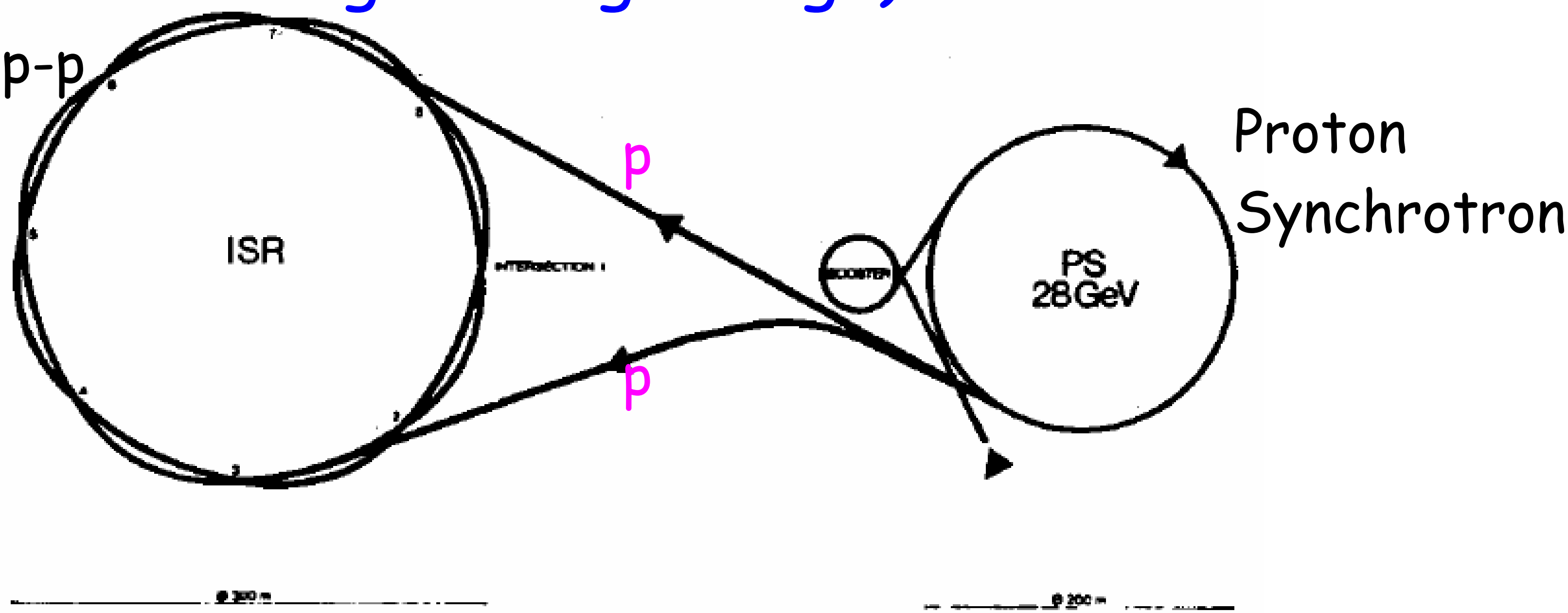

Fig. 2.1. Schematic view of the PS and ISR rings.

ISR: First Publication

Received May 8^{th} 1971

CERN ISR BT/71 11

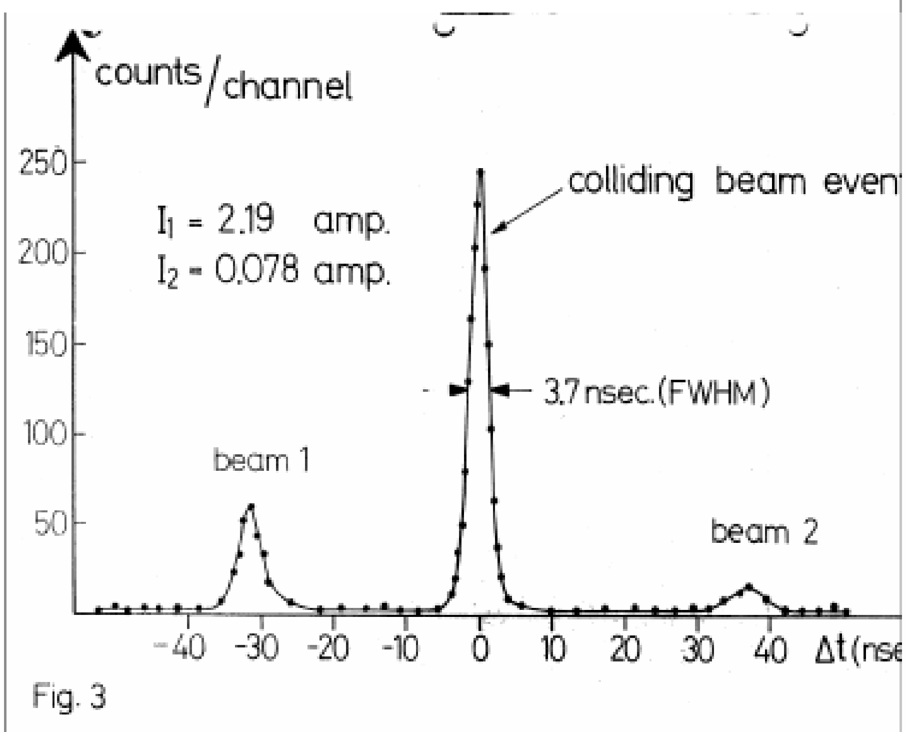

Fig. 3

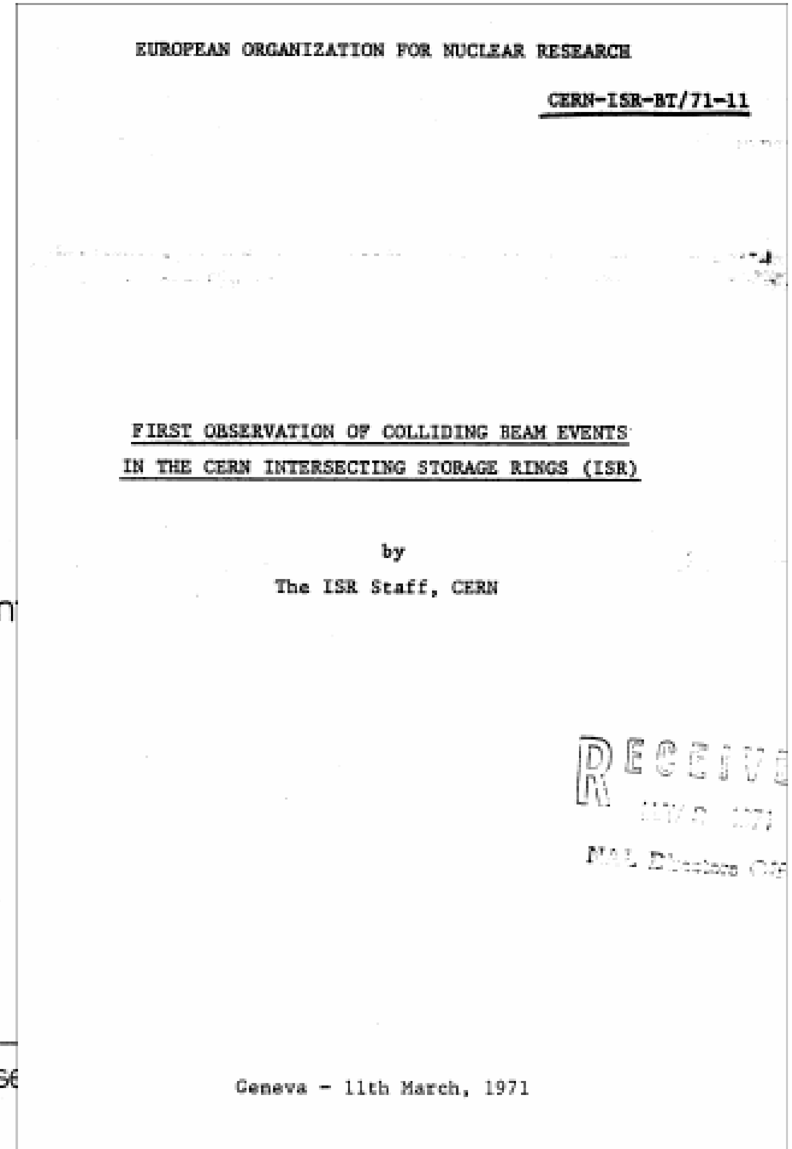

EUROPEAN ORGANIZATION FOR NUCLEAR RESEARCH

CERN-ISR-BT/71-11

FIRST OBSERVATION OF COLLIDING BEAM EVENTS
IN THE CERN INTERSECTING STORAGE RINGS (ISR)

by

The ISR Staff, CERN

RECEIV

Geneva - 11th March, 1971

Hadron Colliders: ISR

Standard Model just at the begin, most phenomenology

π, k, p production cross sections on protons seem constant with E

Most important results:

- measurement of σ(pp), increasing with energy. Later it was determined that all the hadronic cross sections increase at energy of IRS

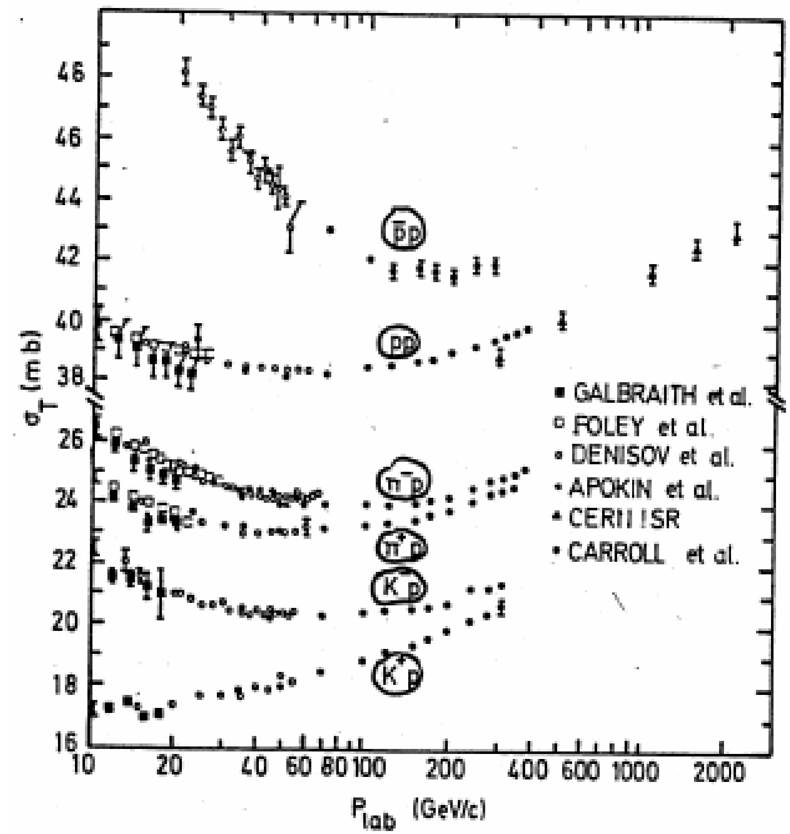

3. Total cross sections on protons. Only momentum dependent errors are shown [4.2].

Hadron Colliders: ISR

Standard Model just at the begin, most phenomenology

π, k, p production cross sections on protons seem constant with E

Most important results:

- measurement of σ(pp), increasing with energy
- determination of dσ/dt (quadri-momentum). It follows optical-diffractive model

Difference of p-p and p-$\bar{p}$ cross section, at high energies goes to zero

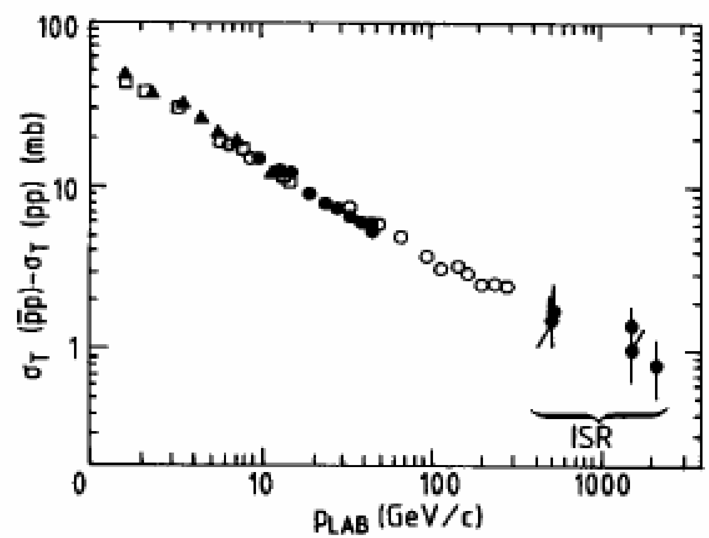

Fig. 43 Measurements of the total cross-section difference, $\sigma_T(p\bar{p})-\sigma_T(pp)$, vs. p_{lab}

Hadron Colliders: ISR

Standard Model just at the begin, most phenomenology

π, k, p production cross sections on protons seem constant with E

Most important results:

- measurement of σ(pp), increasing with energy
- determination of dσ/dt (quadri-momentum). It follows optical-diffractive model
- first hint of jets: excess of secondary tracks at (high) transverse energy

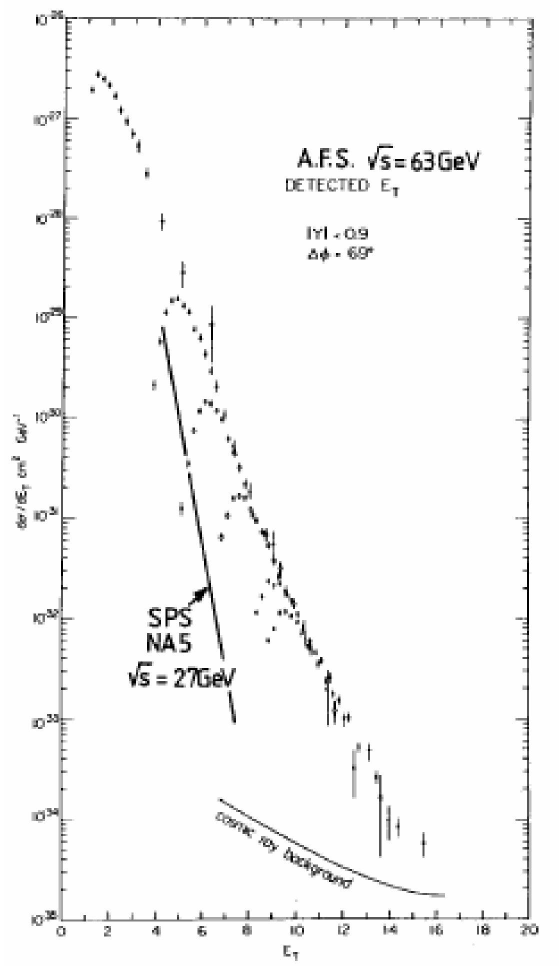

Hadron Colliders: SpS (Super Proton Synchrotron)

1982 CERN was able to produce, accumulate, cool and accelerate pbar thanks to Simon Van der Meer

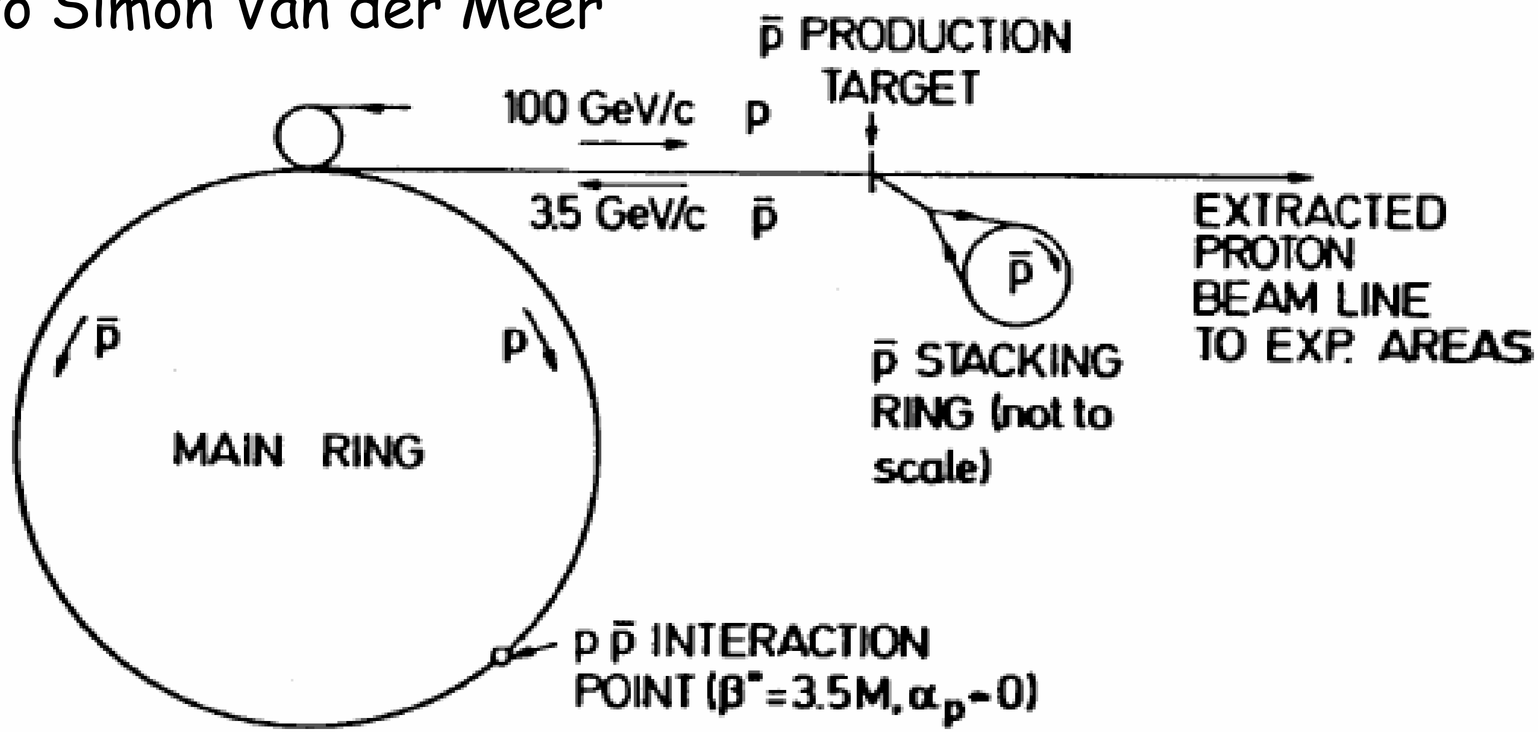

Fig. 5. General layout of the $p\bar{p}$ colliding scheme, from Ref. [9]. Protons (100 GeV/c) are periodically extracted in short bursts and produce 3.5 GeV/c antiprotons, which are accumulated and cooled in the small stacking ring. Then $\bar{p}$'s are reinjected in an RF bucket of the main ring and accelerated to top energy. They collide head on against a bunch filled with protons of equal energy and rotating in the opposite direction.

UA1 and UA2 Detectors

The detectors UA1 & UA2

Underground Area 1,2: 35 meters underground

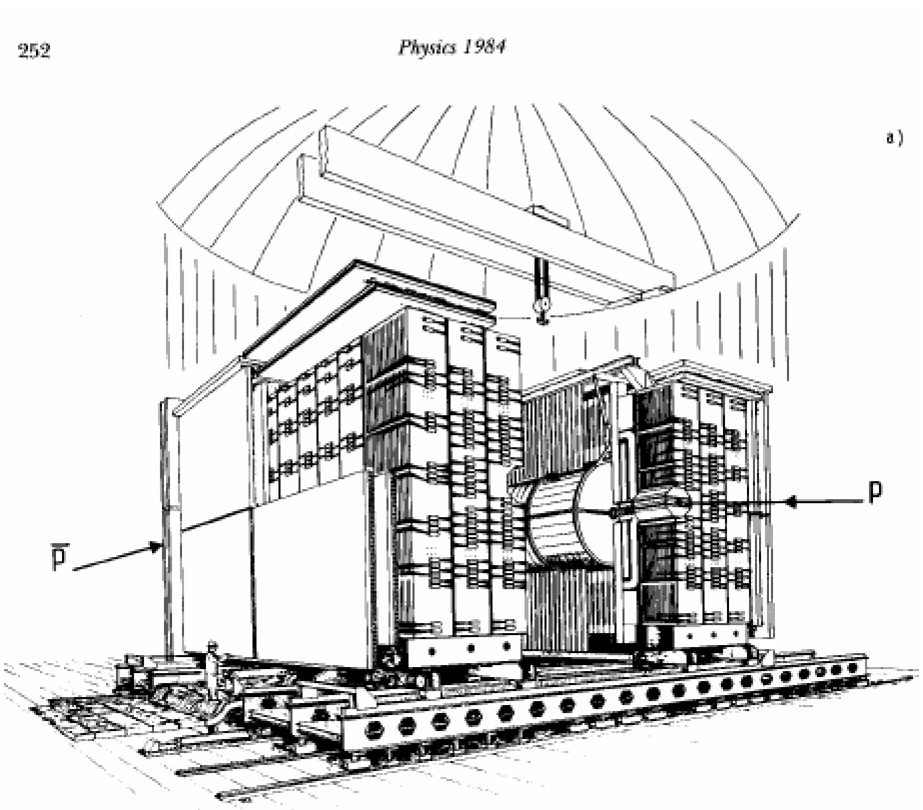

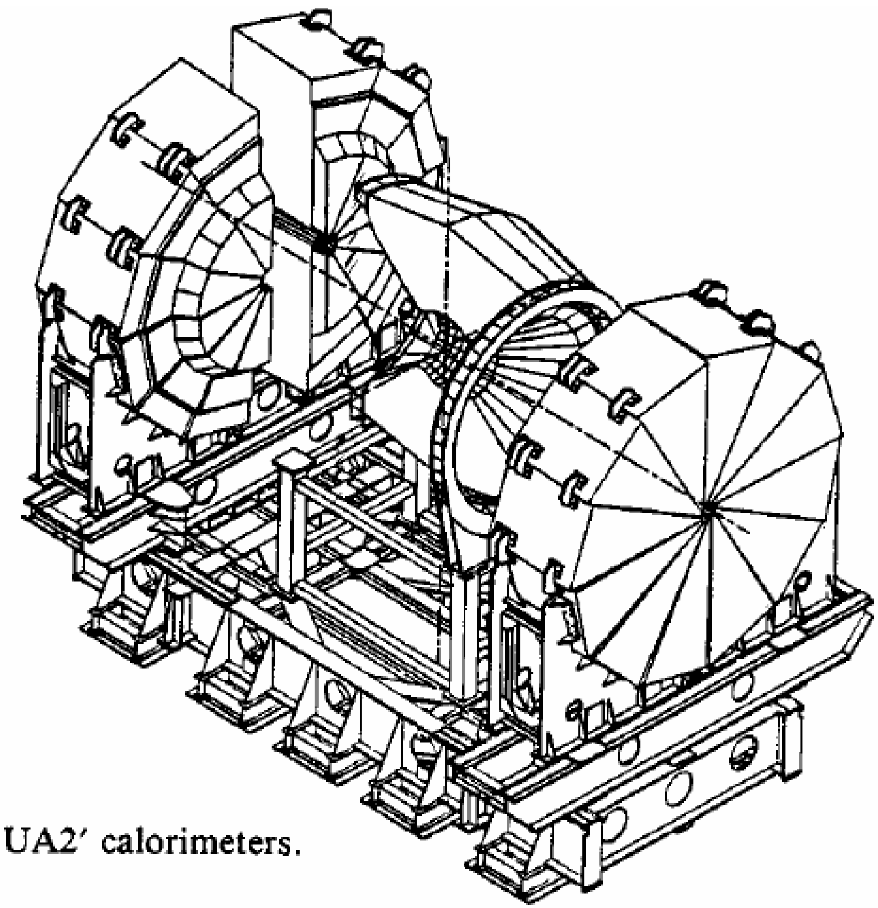

'the UA2' calorimeters.

SpS Results

The Standard Model is a reality:
- jets identification
- measurements of hadronic cross section
- discovery of W and Z bosons

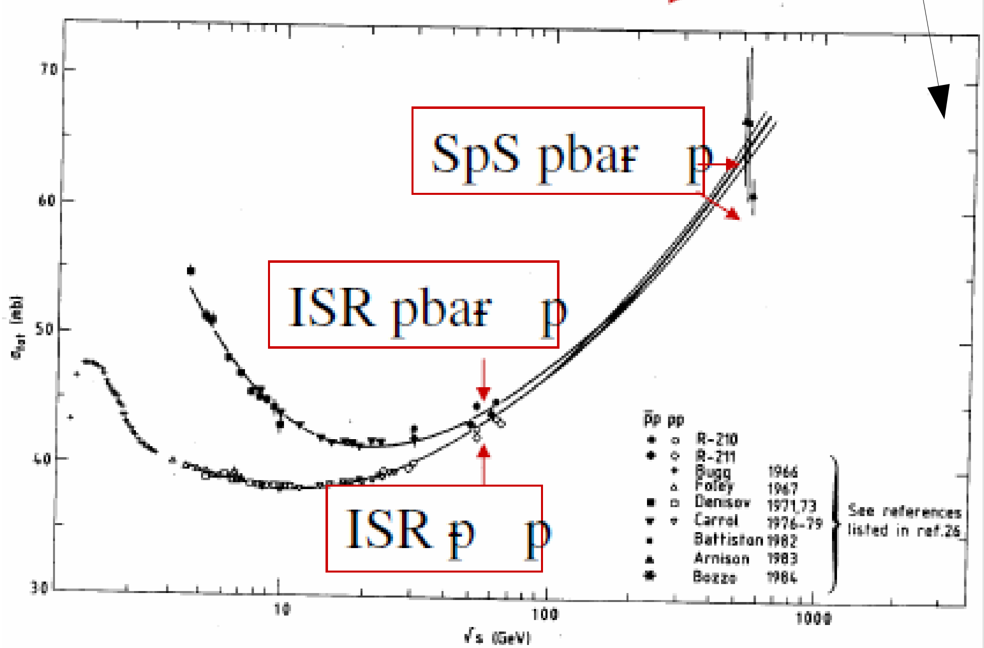

Fig. 7. The behaviour of $\sigma_{tot}(pp)$ and $\sigma_{tot}(\bar{p}p)$ as a function of $\sqrt{s}$.

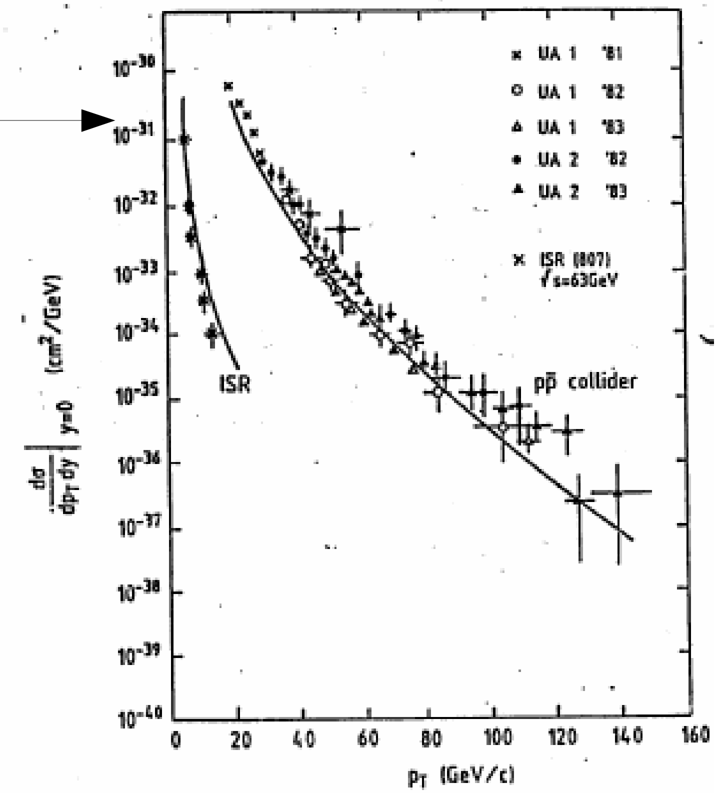

ISR just
under threshold
for jets production

SpS Results: W discovery

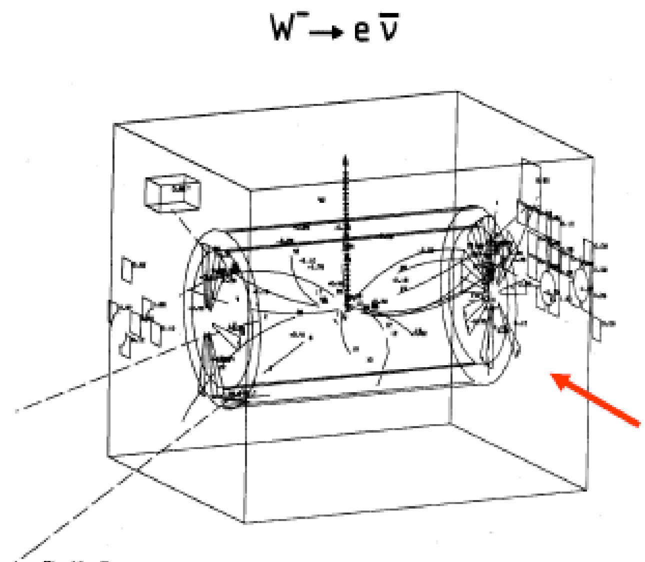

Fig. 16a. Event of the type $W^- \rightarrow e^- + \bar{\nu}_e$. All tracks and calorimeter cells are displayed.

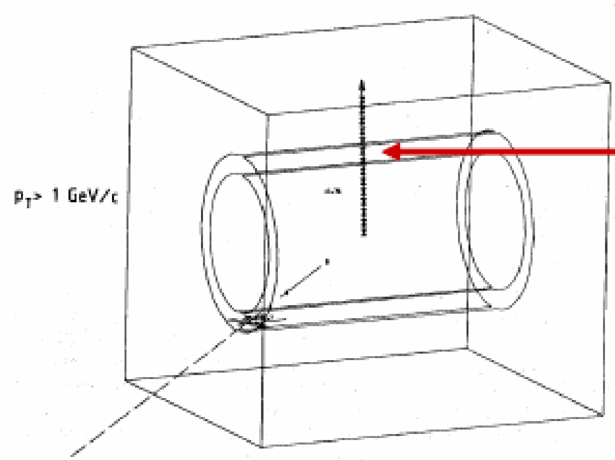

Fig. 16b. The same as picture (a), except that now only particles with $p_T > 1$ GeV/c and calorimeters with $E_T > 1$ GeV are shown.

First W candidate

Showing all tracks it is difficult to declare it is a W

Cutting tracks with E<1GeV there is only the e

UA2 demonstrated that these events were W comparing to expectations

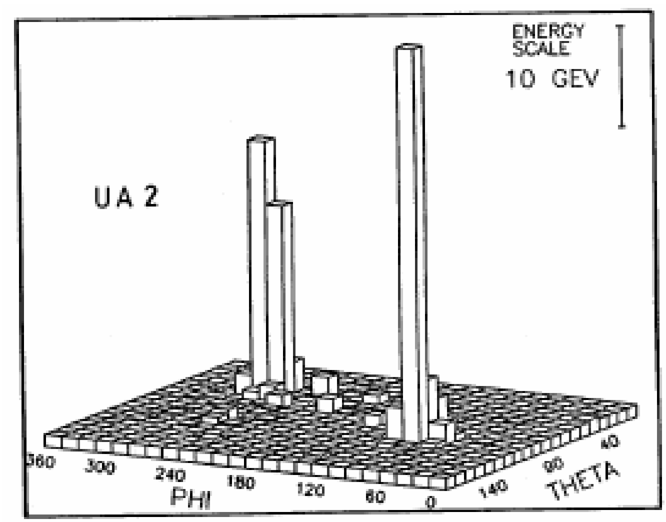

The highest E_T event of Fig. 9, showing the E_T distribution in θ and ϕ

SpS Results: W & Z discovery

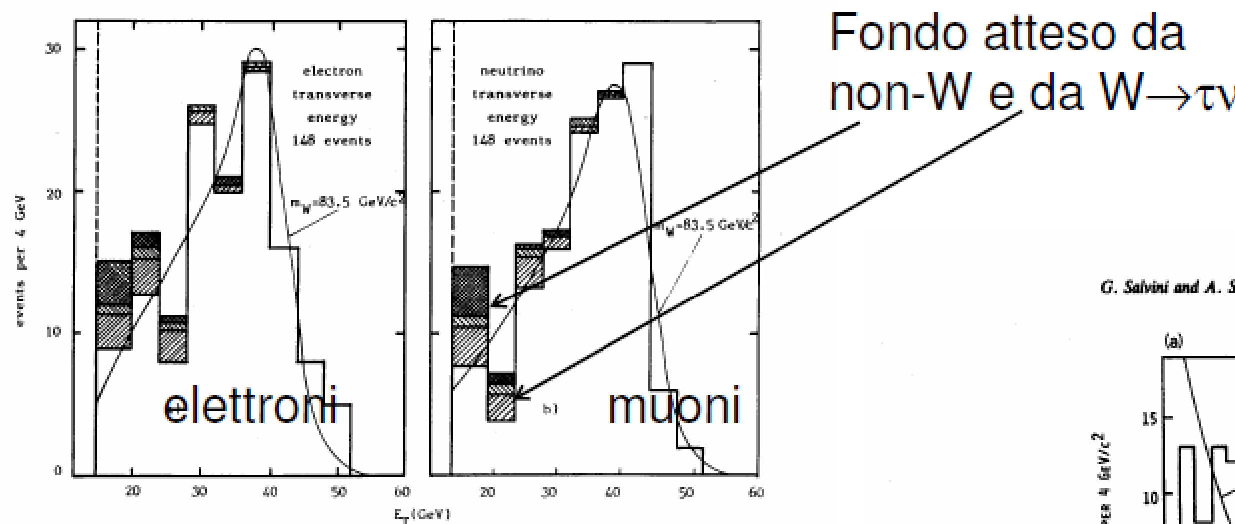

Fig. 3.5. The lepton transverse energy distributions for the UA1 sample of well-measured $W^{\pm}\to e^{\pm}\nu_e$ events, (a) the electron transverse energy distribution and (b) the neutrino transverse energy distribution. The shaded parts show the expected contributions from jet–jet fluctuations (cross-hatched) and $W\to\tau\nu$ decays with $\tau\to$ hadrons (top left to bottom right hatching) and $\tau\to e\nu_e\nu_\tau$ (top right to bottom left hatching). The curves show the predictions for the background subtracted distributions (normalized to the data) corresponding to W with a mass of 83.5 GeV/c^2. Transverse energy and transverse momentum are in this case equivalent expressions (UA1 [21]).

e+e- invariant: the Z^0

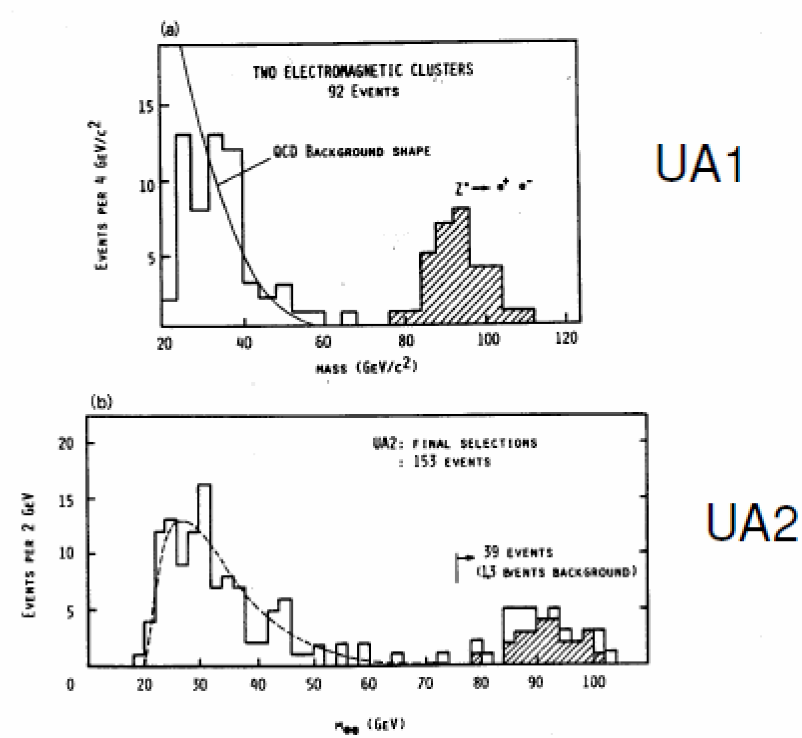

Fig. 3.9. (a) The distribution of e^+e^- pairs, recognized as $Z^0\to e^+e^-$ processes (UA1 [21]). (b) The e^+e^- events, collected by UA2 [22].

Hadron Colliders: Tevatron

The first super-conducting syncroton
Electric field to accelerate particles
Magnetic field to drive and focus particles
using dipoles and quadrupoles

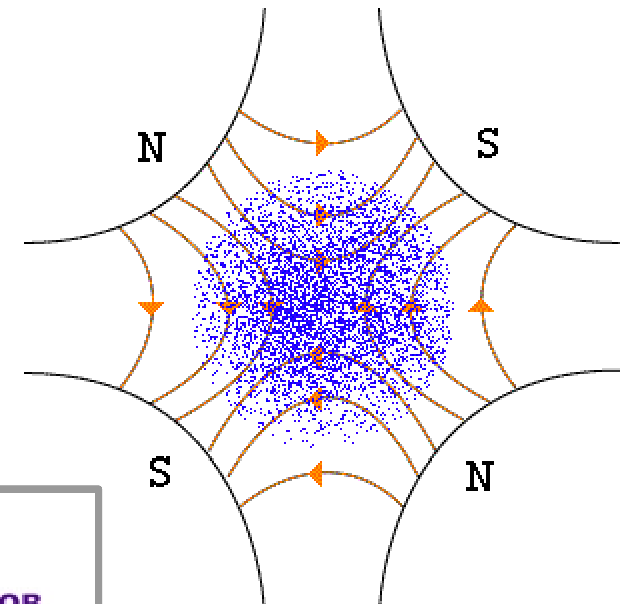

Complex chain:

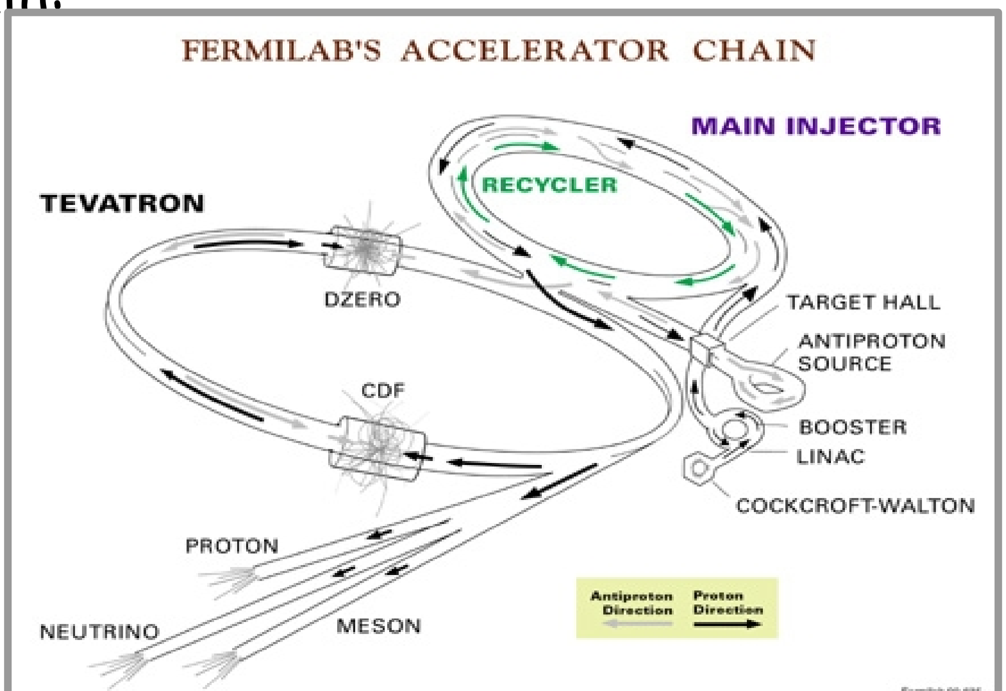

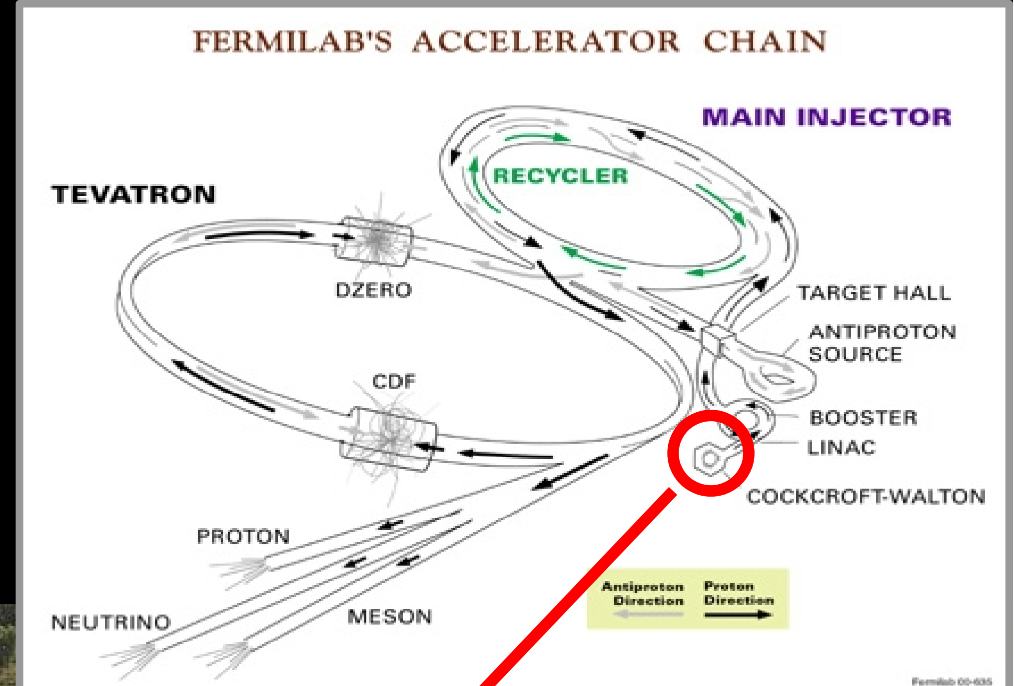

Cockroft-Walton accelerator:
H^- ions produced and accelerated up to **750 keV**

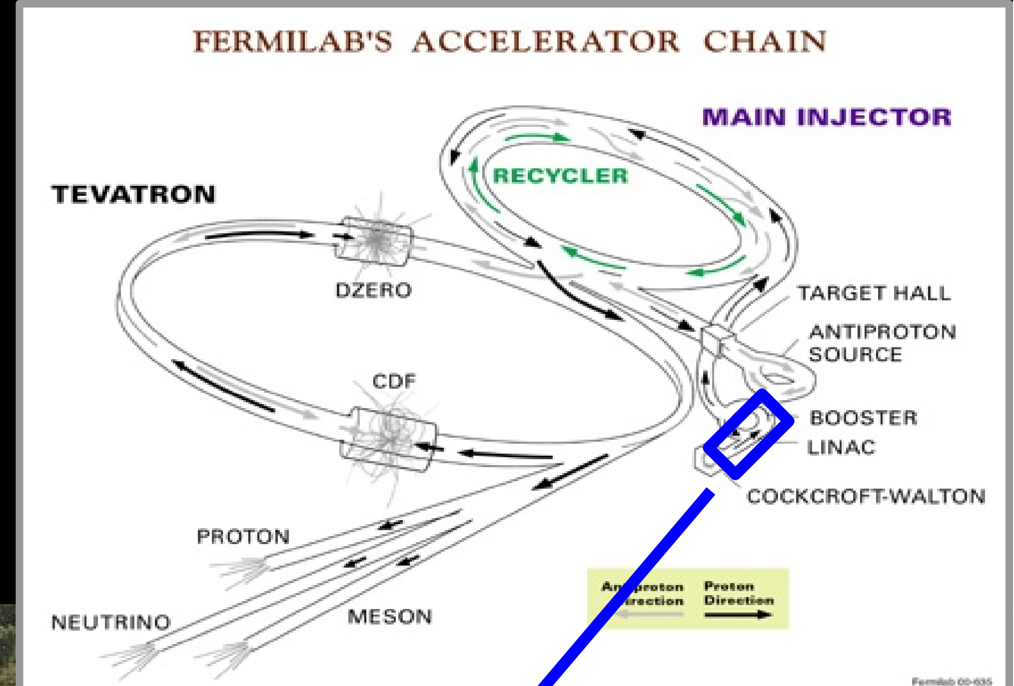

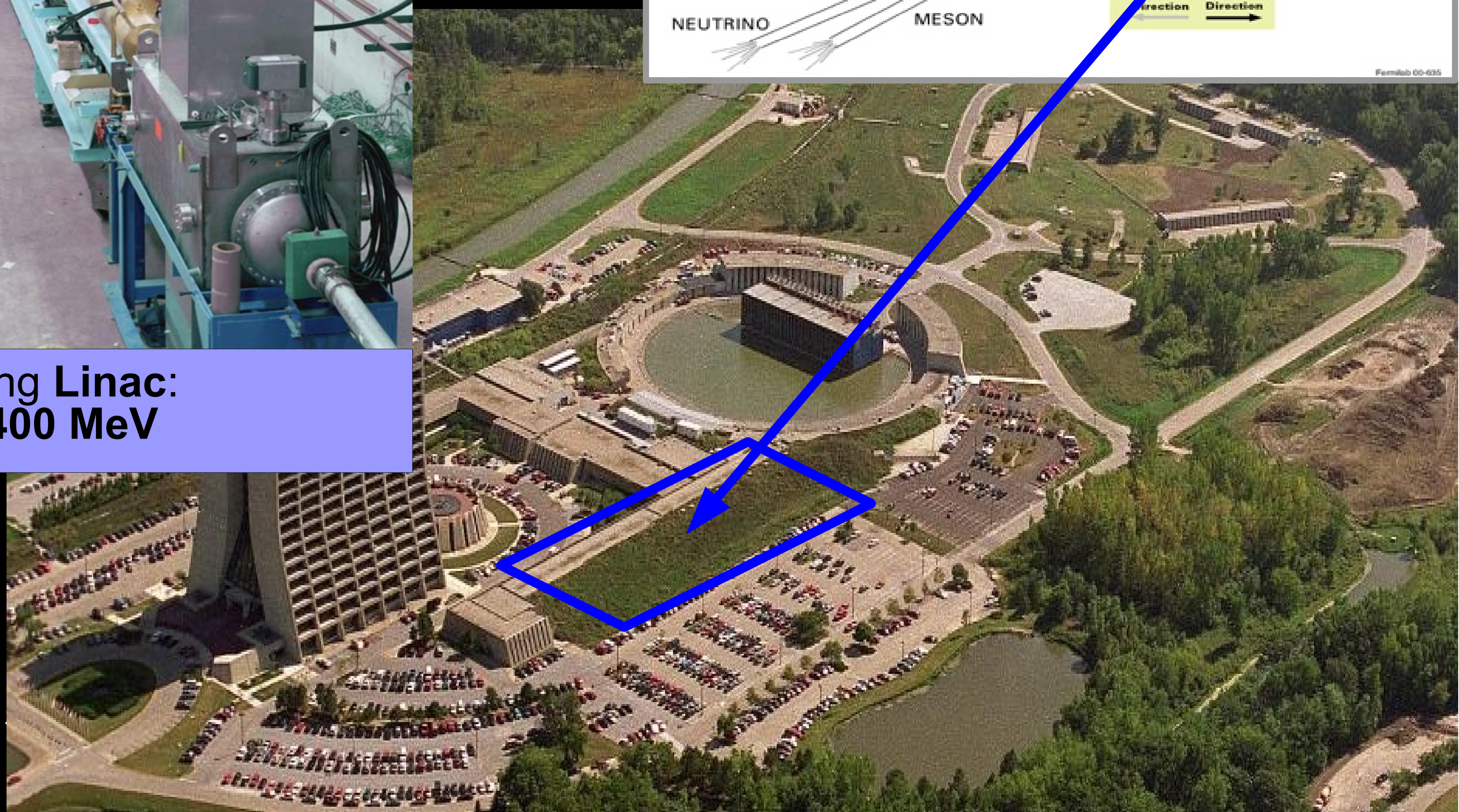

150 m long **Linac**:
H^- up to **400 MeV**

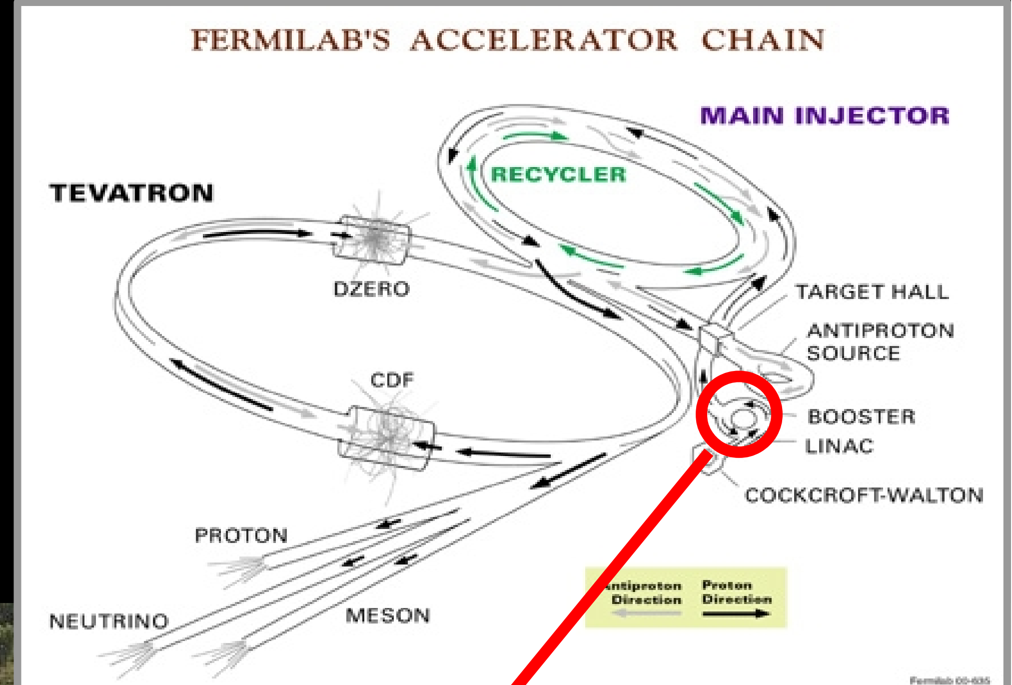

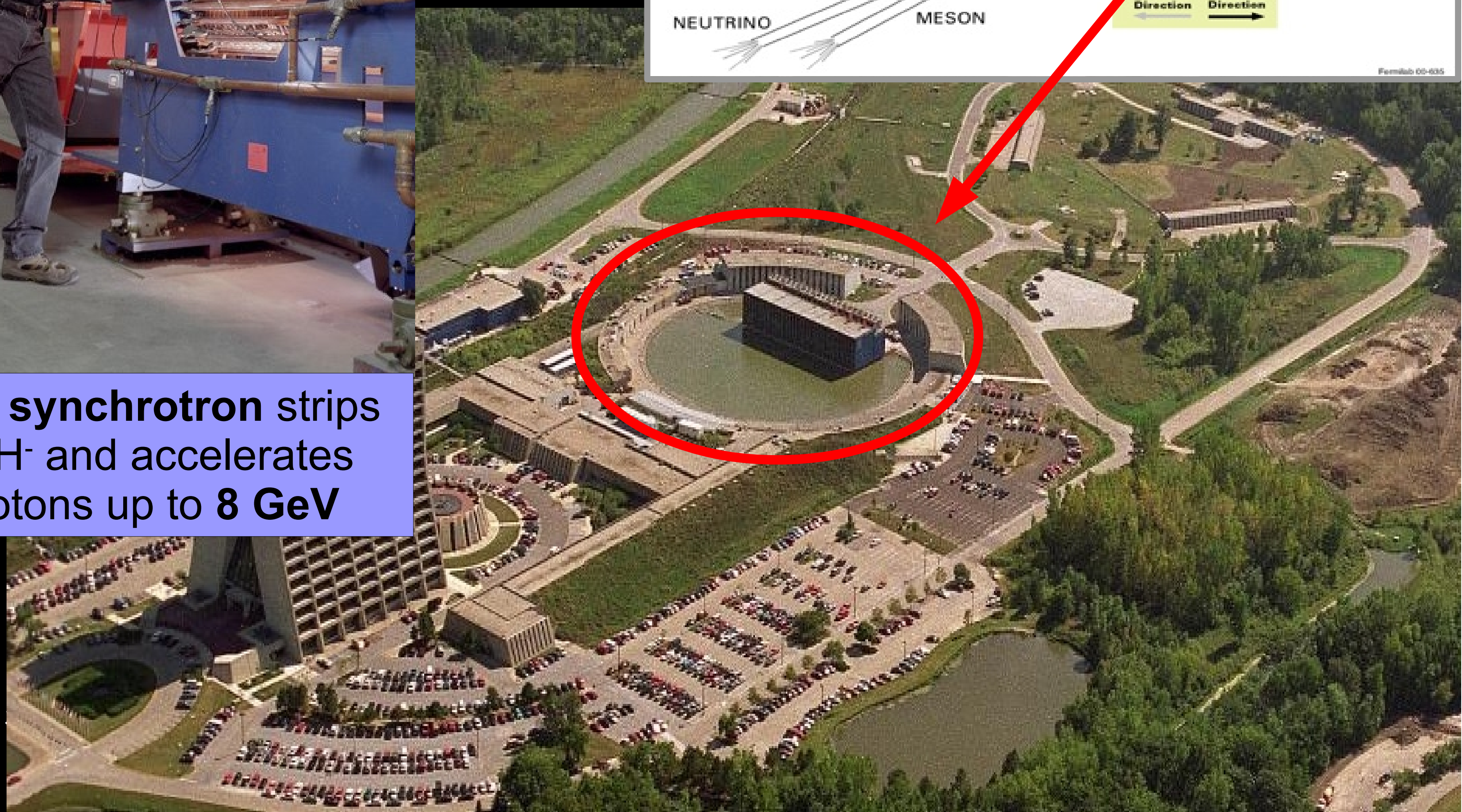

The **Booster synchrotron** strips electrons off H^- and accelerates remaining protons up to **8 GeV**

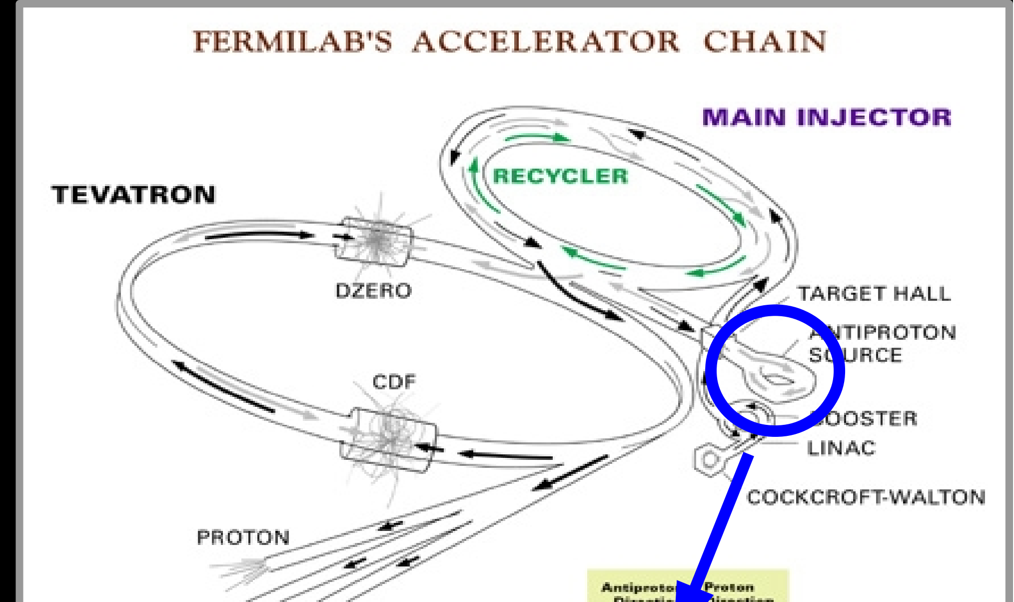

The Anti-proton Source

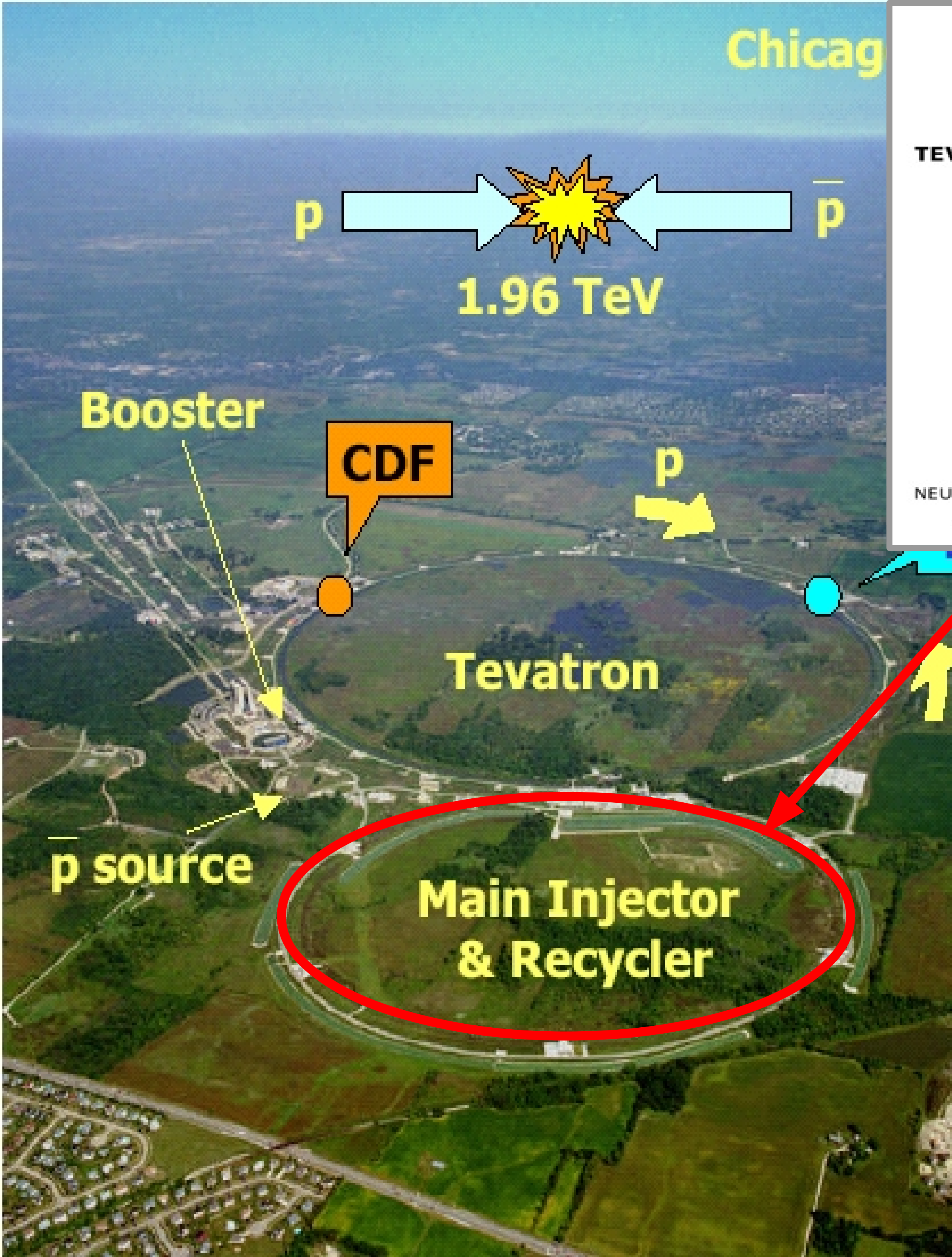

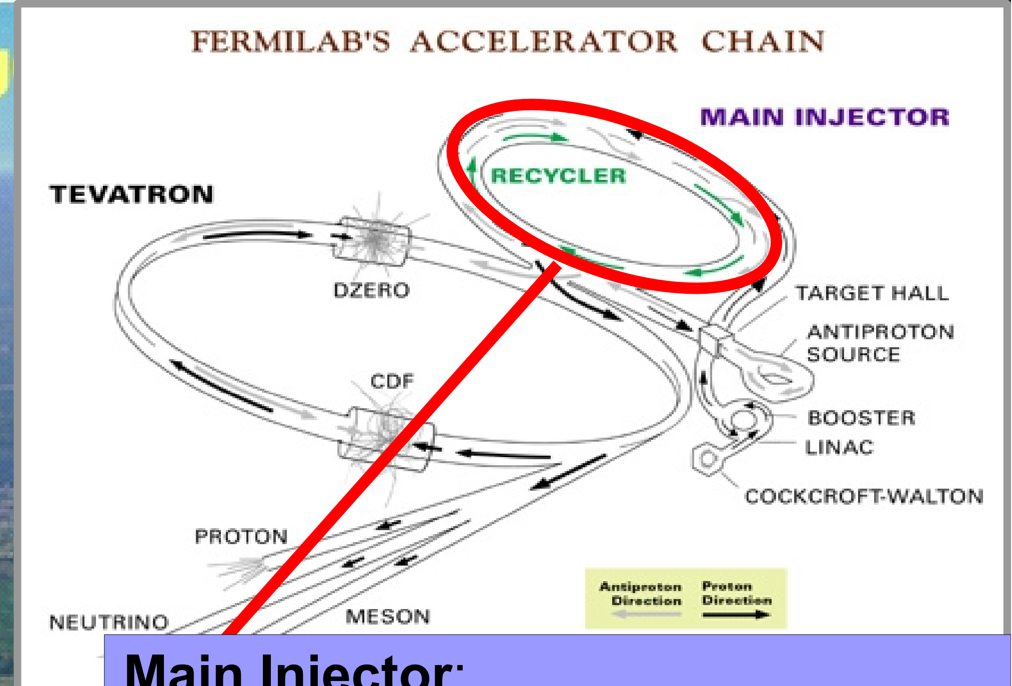

Main Injector:

- p up to **120 GeV** for anti-p prod.
- deliver p-beams to fixed target exp
- accelerate p/anti-p up to **150 GeV** for Tevatron Injection.
- send to recycler anti-p after stores

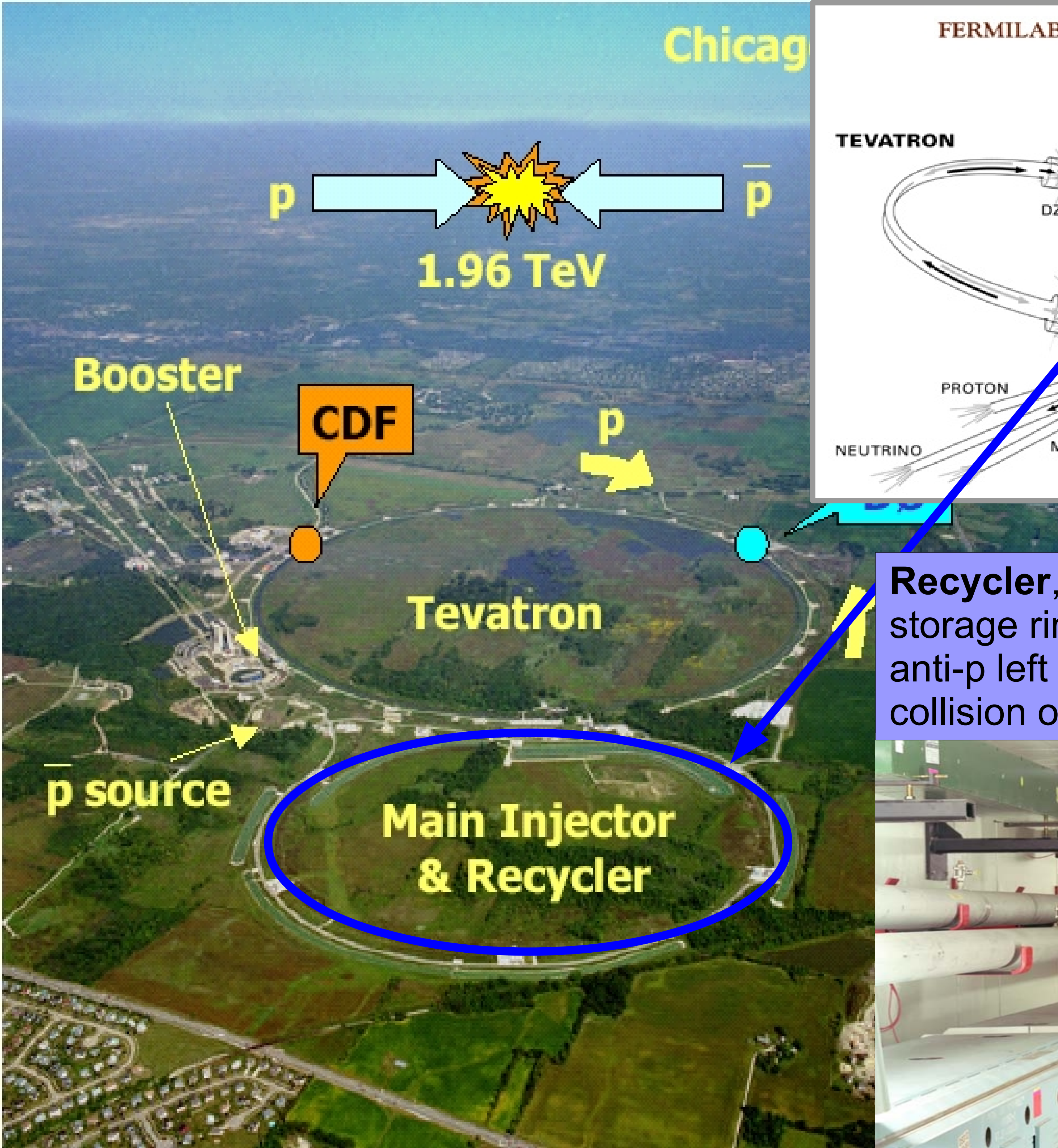

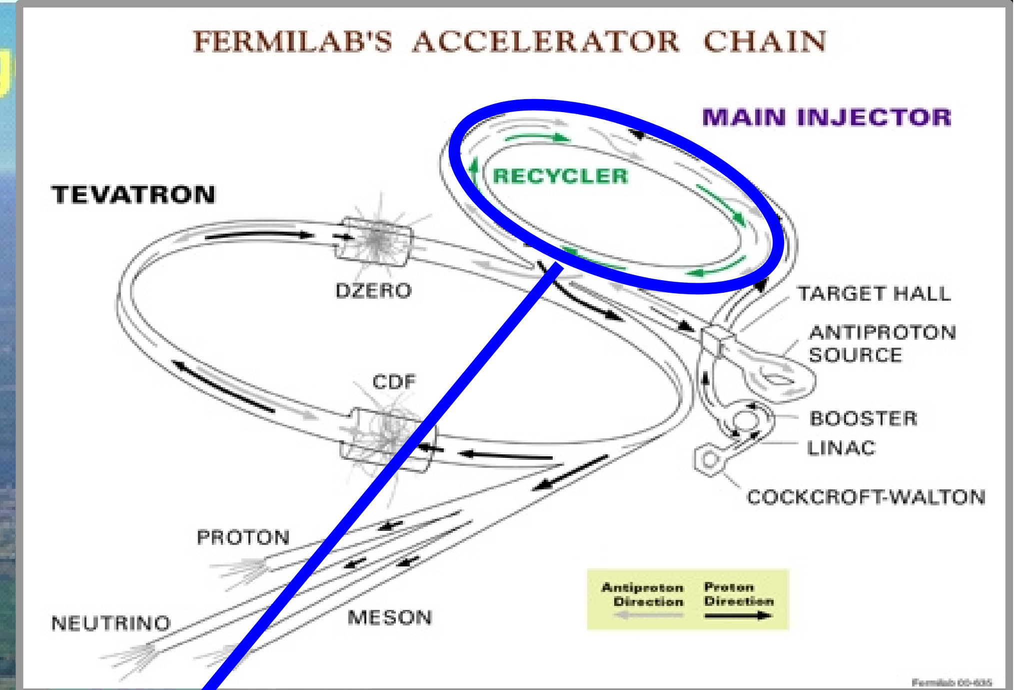

Recycler, **8 GeV** fixed energy storage ring: recover and recool anti-p left over after Tevatron collision operations

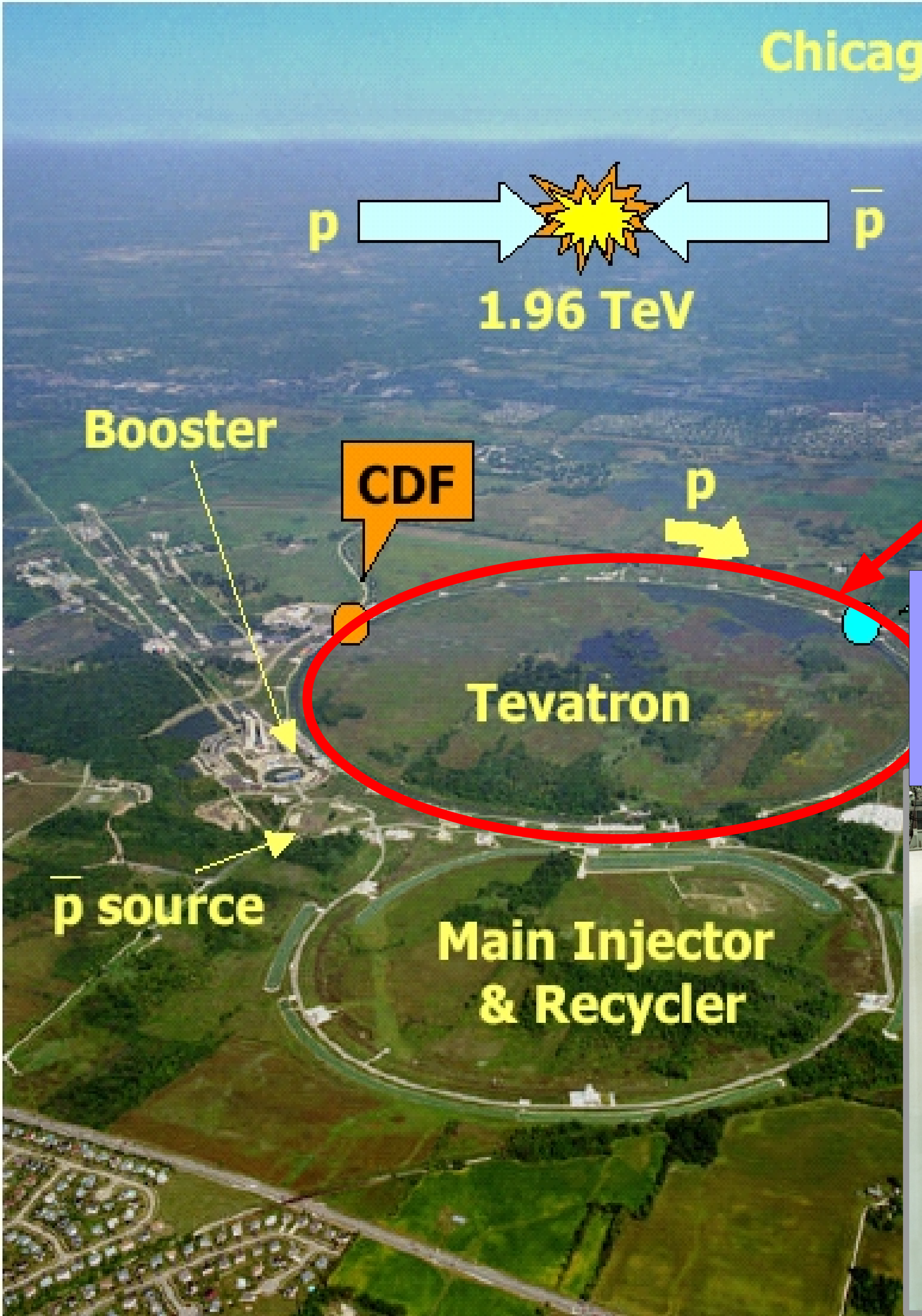

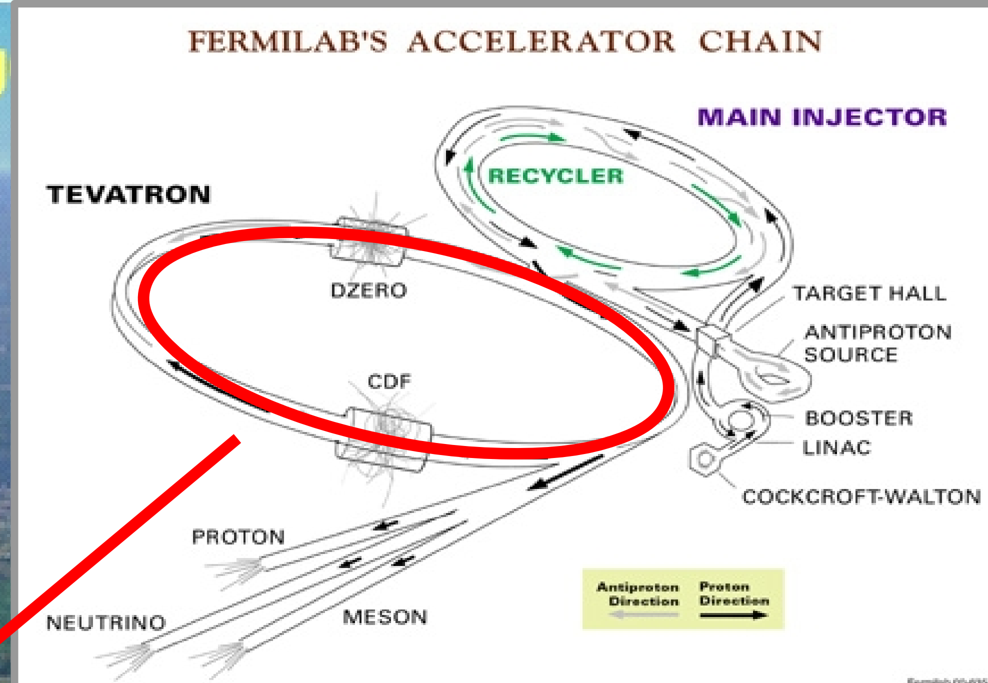

Tevatron:
p/anti-p beams up to **980 GeV,**
providing a
center of mass energy of **1.96 TeV**

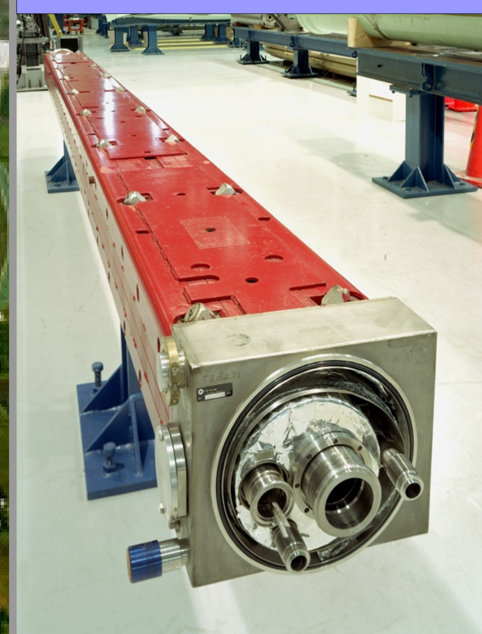

Tevatron bunch structure

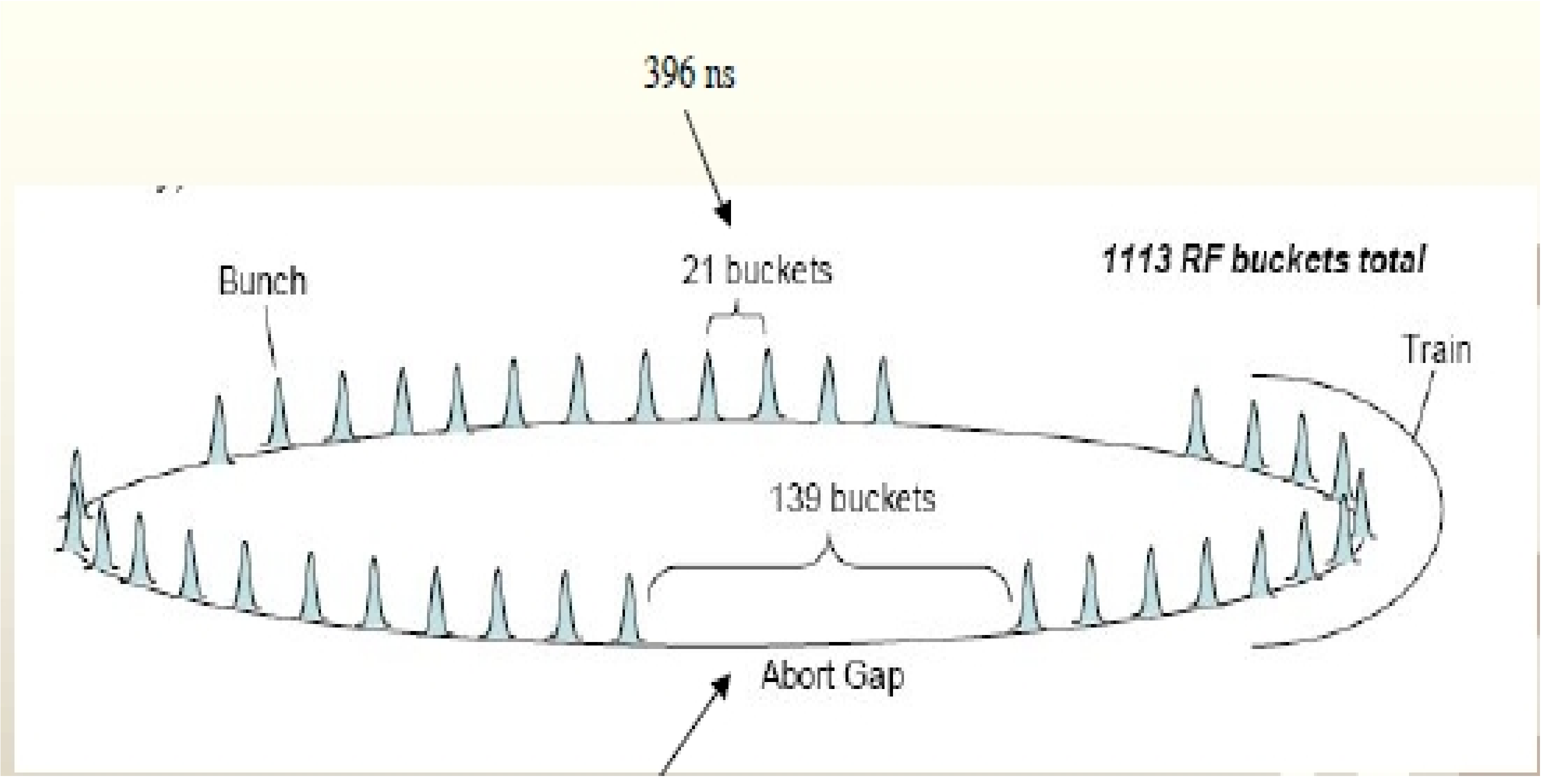

2.6μs

The new hadron Colliders: LHC

1982 : First studies for the LHC project

1983 : Z0/W discovered at SPS proton antiproton collider (SppbarS)

1989 : Start of LEP operation (Z/W boson-factory)

1994 : Approval of the LHC by the CERN Council

1996 : Final decision to start the LHC construction

2000 : Last year of LEP operation above 100 GeV

2002 : LEP equipment removed

2003 : Start of LHC installation

2005 : Start of LHC hardware commissioning

2008 : Start of (short) beam commissioning Powering incident on 19th Sept.

2009 : Repair, re-commissioning and beam commissioning

2010 : LHC starts again after technical stop and first collisions at 7 TeV

2012 : Higgs discovery

2013 : First long shutdown

2015 : LHC back in bussines at 13 TeV

The new hadron Colliders: LHC

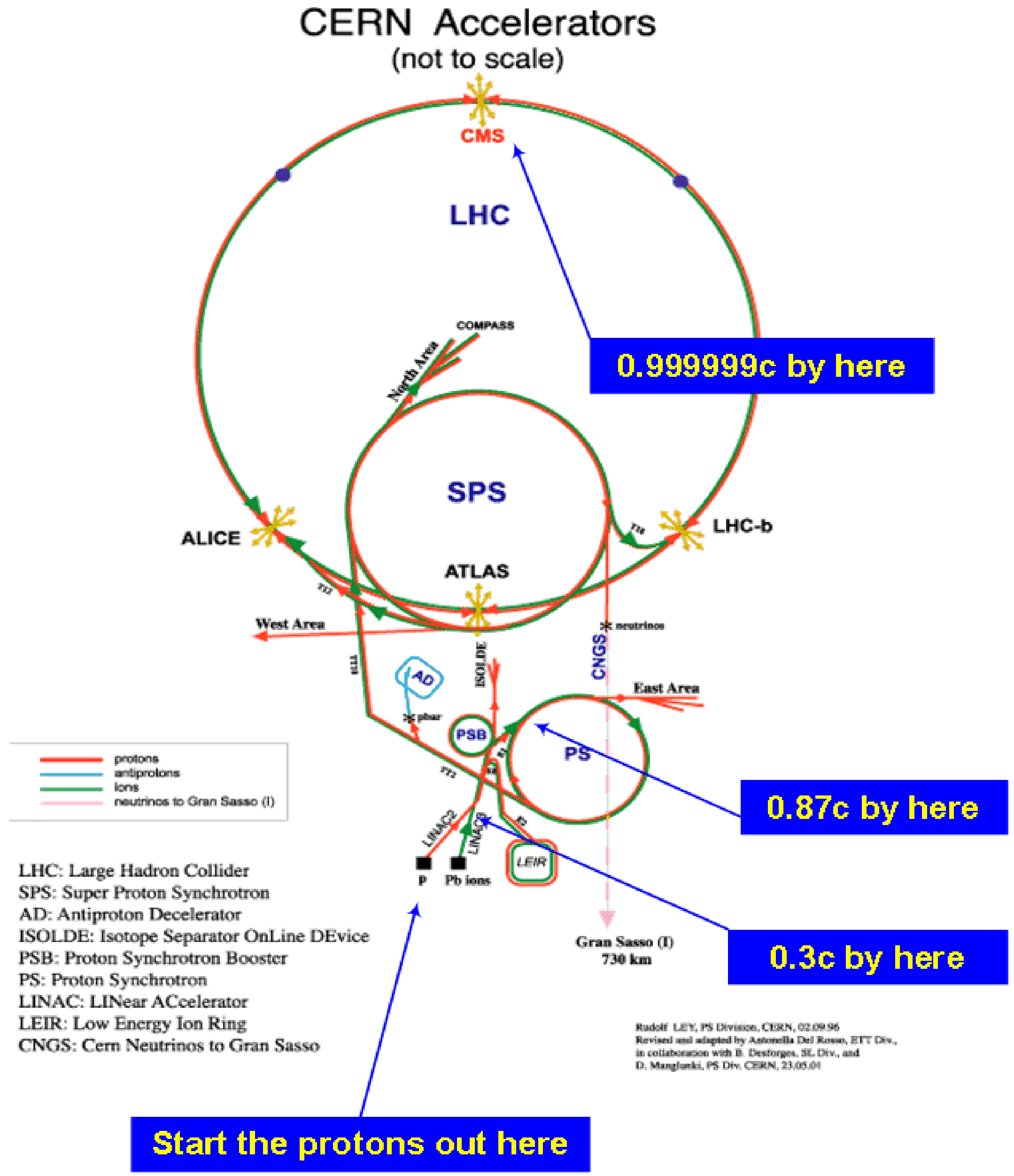

The new hadron Colliders: LHC

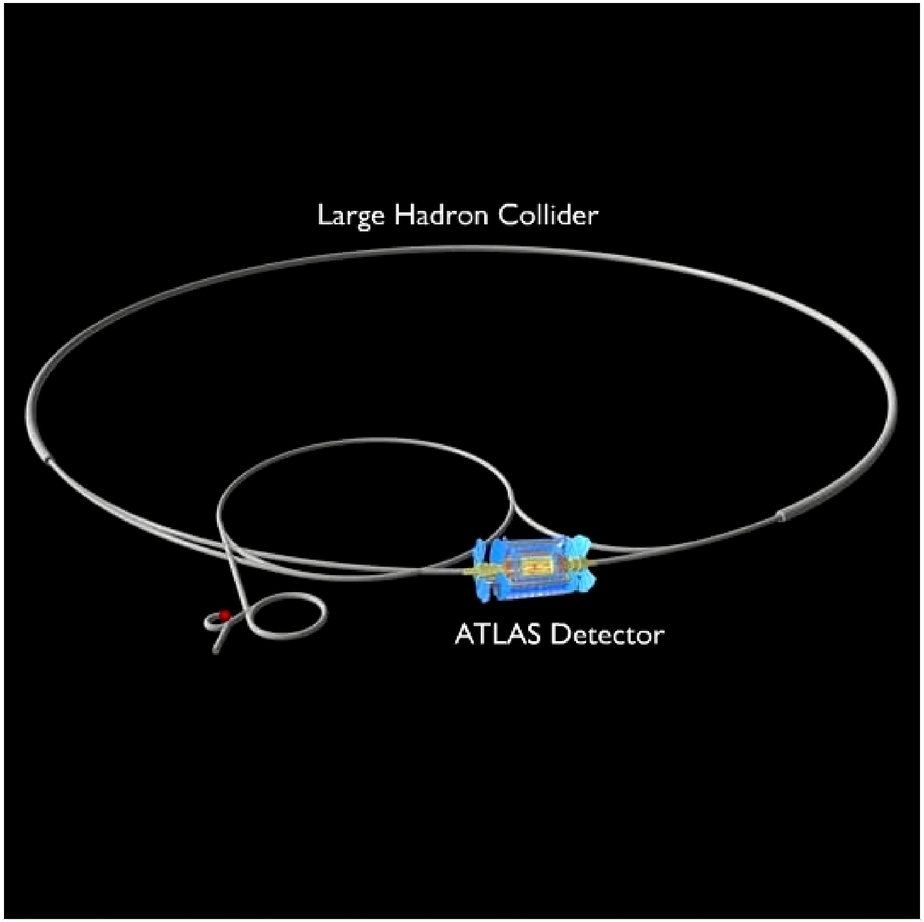

How particles interacts with matters

Particles interacts with matter depending on the type of particle and the energy.

We use the energy deposited by the particle to identify the it.

Charge Particle → collision with atoms and atomic e → ionization and excitation of atoms

Neutral particle → interaction with material → charge particle production → ionization and excitation of atoms

Summary of the energy loss mechanisms:

- multiple scattering
- Bethe-Block
- $e^{\pm}$
- photons

Bethe-Block

The mean energy loss of a charged particle:

$$-\frac{dE}{dx} = \rho 4\pi N_0 r_e^2 mc^2 \frac{Z}{A} z^2 \frac{1}{\beta^2}\left[\frac{1}{2}\ln\frac{2mc^2\beta^2\gamma^2 T_{\max}}{I^2} - \beta^2 - \frac{\delta(\gamma)}{2}\right]$$

1. It depends on the charge of the incident particle (z^2)
2. It depends on the average excitation potential of the material (I)
3. It goes as $1/\beta^2$ for increasing β with a minimum around $\beta\gamma \sim 3 \div 4$ which is almost the same for all particles of the same charge, then grows again ($\log(\beta^2\gamma^2)$ dominates) relativistic rise
4. The relativistic raise stops and it reaches a plateau (Fermi plateau)

Bethe-Block

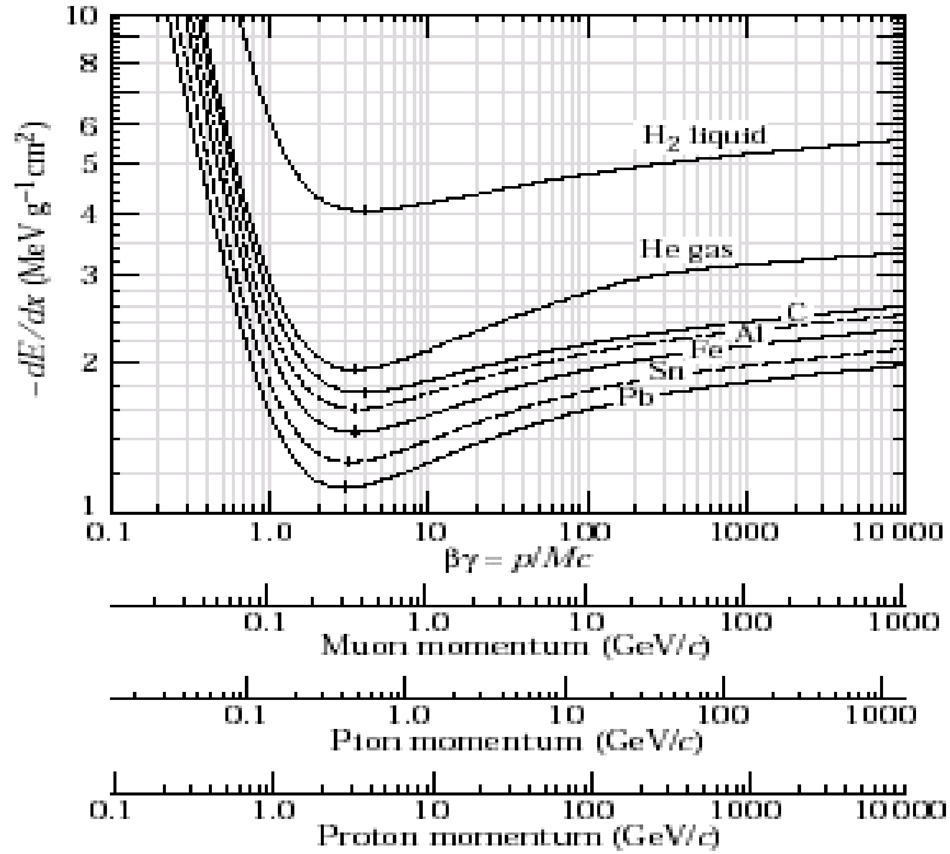

Figure 26.3: Mean energy loss rate in liquid (bubble chamber) hydrogen, gaseous helium, carbon, aluminum, iron, tin, and lead. Radiative effects, relevant for muons and pions, are not included. These become significant for muons in iron for $\beta\gamma \gtrsim 1000$, and at lower momenta for muons in higher-Z absorbers. See Fig. 26.20.

Energy loss fluctuations

Thick absorber: many interactions → the energy loss is distributed as a Gaussian.

Thin absorber: Landau distribution or/and Vavilov distribution

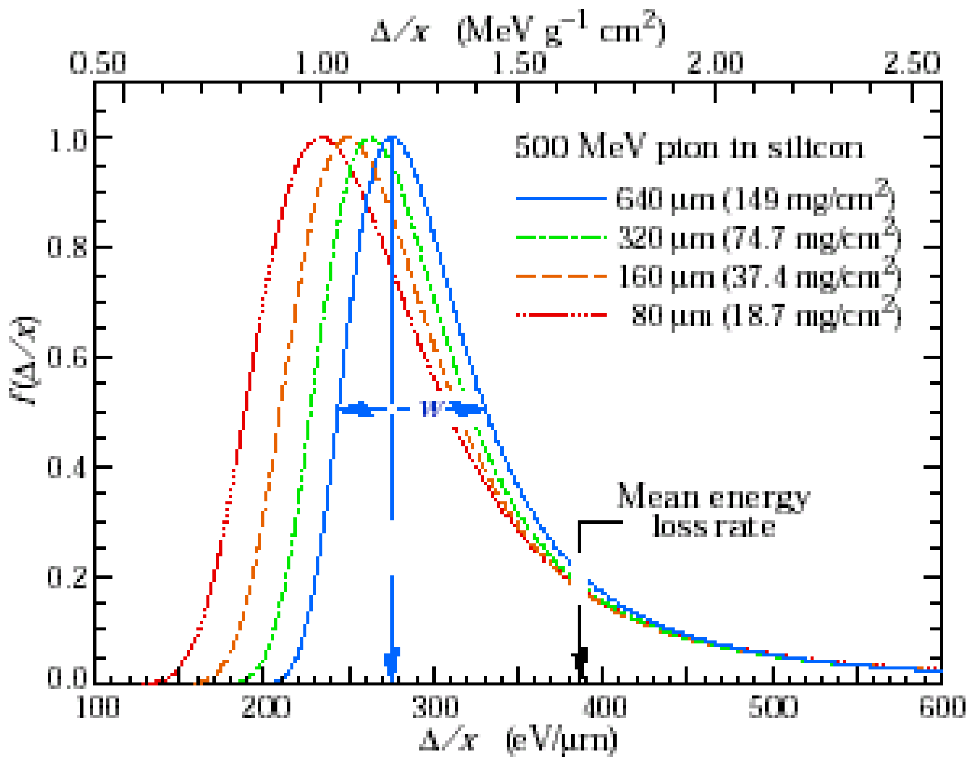

Cerenkov Effect

The Cerenkov radiation is emitted when a charged particle moves in a material medium faster than the speed of light in the same material, $\beta c = v > c/n$ where v is the speed of the particle and n is the index of refraction of the material.

The light is emitted at fixed angle

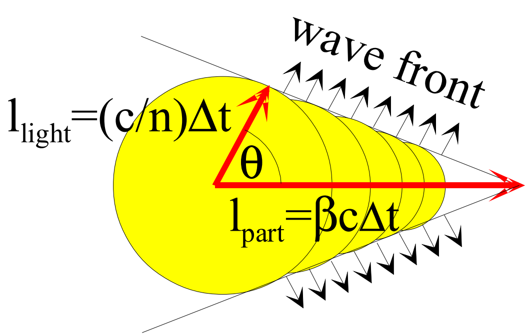

$$\cos\theta_C = \frac{1}{n\beta} \quad \text{with} \quad n = n(\lambda) \geq 1$$

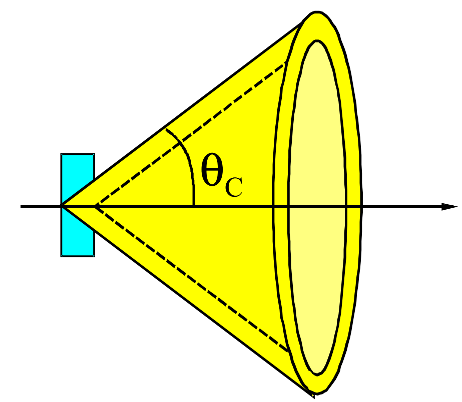

Cerenkov Effect

The number of photons emitted per unit length and unit wavelength:

$$\frac{d^2N}{dxd\lambda} = \frac{2\pi z^2\alpha}{\lambda^2}\left(1 - \frac{1}{\beta^2 n^2}\right) = \frac{2\pi z^2\alpha}{\lambda^2}\sin^2\theta_C$$

$$\frac{d^2N}{dxd\lambda} \propto \frac{1}{\lambda^2} \quad \text{with} \;\; \lambda = \frac{c}{\nu} = \frac{hc}{E} \qquad \frac{d^2N}{dxdE} = const.$$

It decreases as function of wavelength

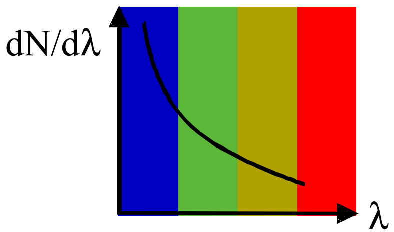

It is constant as function of E

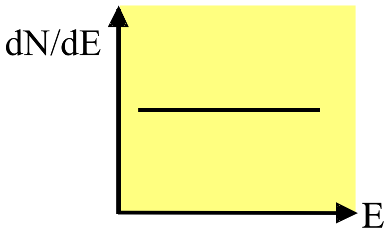

Electrons energy loss

Electrons and positrons lose energy by collisions with material atoms described by the Bethe-Block formula (modified) and by Bremsstrahlung.

$(dE/dx)_{tot} = (dE/dx)_{rad} + (dE/dx)_{coll}$

The critical energy E_c is defined $(dE/dx)_{rad} = (dE/dx)_{coll}$

$E_c = 800(\mathrm{MeV})/(Z+1.2)$

For high values of γ ($E>E_c$) the dominant process is the Bremsstrahlung:

$dE/dx = E/X_0$ from which: $E = E_o e^{-x/X_o}$

that defines the radiation length:

after a legth $x = X_0$ the energy drops by 1/e

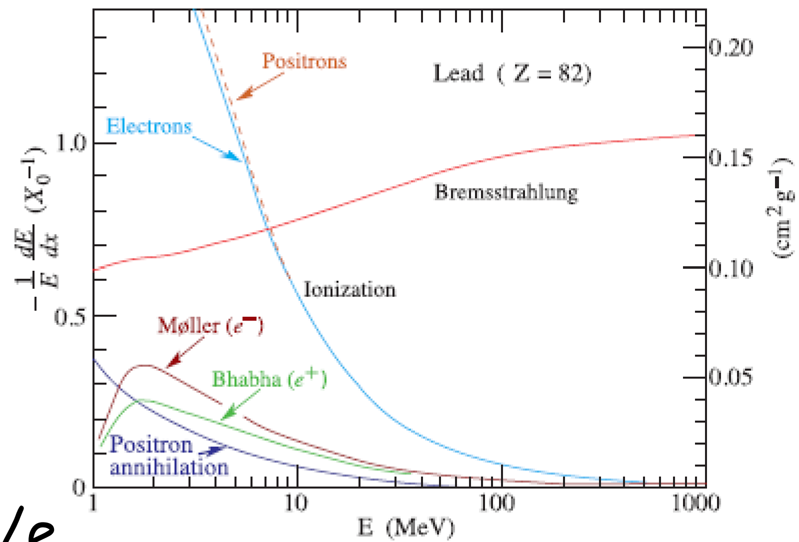

Multiple Scattering

Elastic scattering of particle on nucleus material, the particle does not lose energy but changes direction (Coulomb scattering)

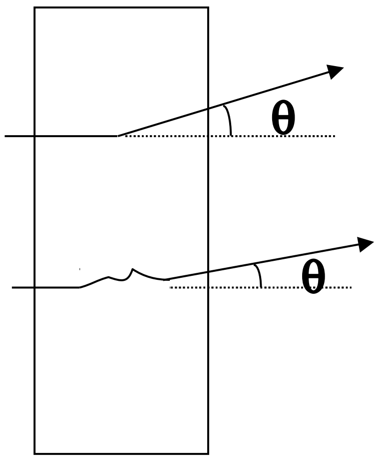

The average angle of scattering is zero in the multiple scattering but the dispersion can be calculated

$$\langle \theta^2_{ms} \rangle = \frac{x}{X_0} \frac{4\pi}{\alpha} \frac{m^2}{\beta^2 p^2}$$ as function of energy

X_0 = radiation length

$$\theta_{ms} = \frac{E_s}{\beta c p} \sqrt{x X_0} \qquad \left(E_s = \sqrt{\frac{4\pi}{\alpha}} \cdot mc^2 \approx 21\, MeV \right)$$

If the particle goes through a "small" number of X_0 more accurate:

$$\theta_{ms} = \frac{19.2}{\beta c p} [MeV] \sqrt{x / X_0} \left(1 + 0.038 \ln \left({}^{x}\!/_{X_0} \right) \right)$$

When the particle hits the nucleus electron → small particle deviation

Possible e extraction (delta rays)

Photons energy loss

Photons interact with matter via:

- photoelectric effect
- Compton effect
- pairs production

At high energy the pairs production dominates

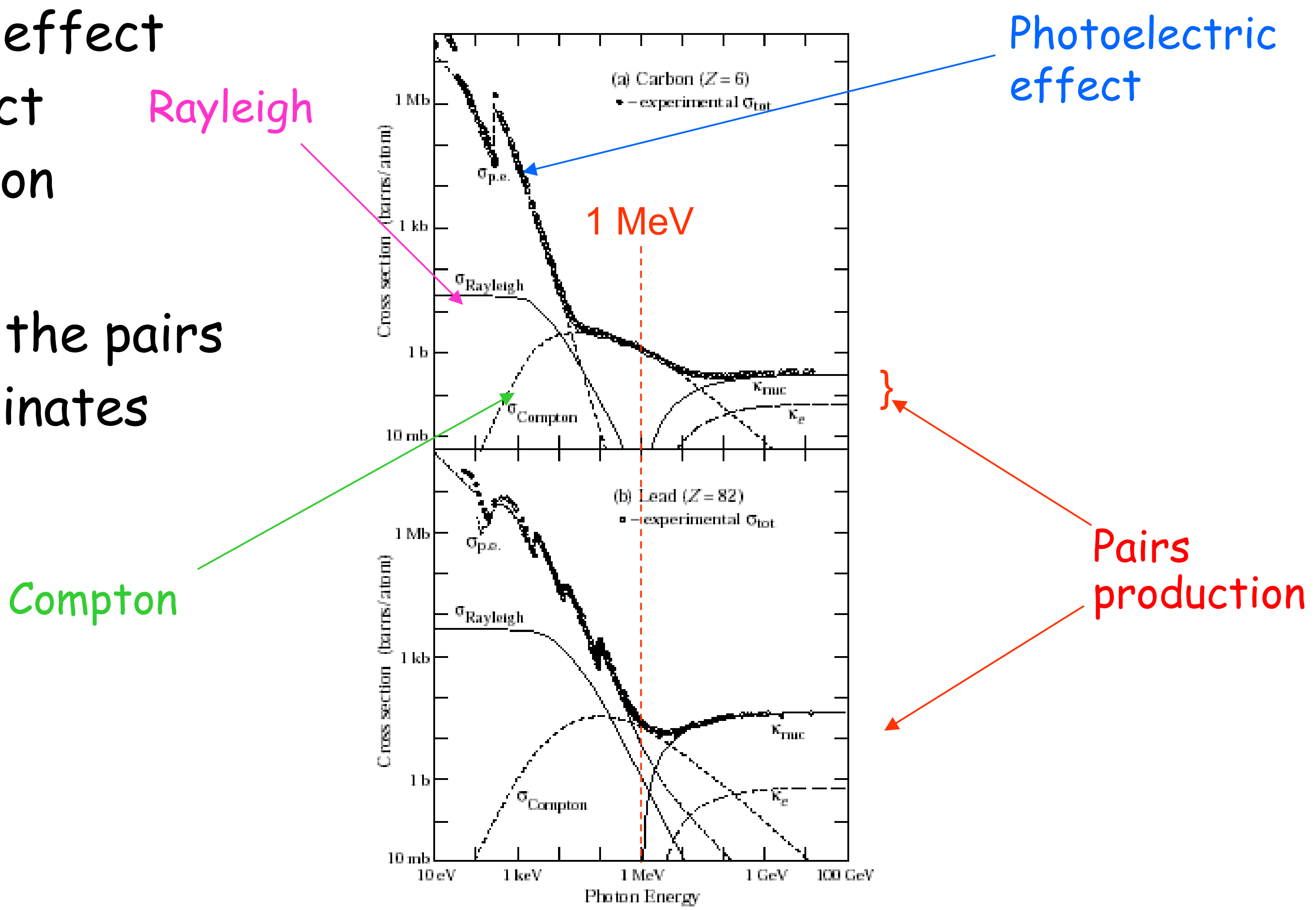

Electromagnetic Showers

Combining what we have seen on $e^{\pm}$ and γ interaction we can understand how high energy em particles interact with matter forming showers

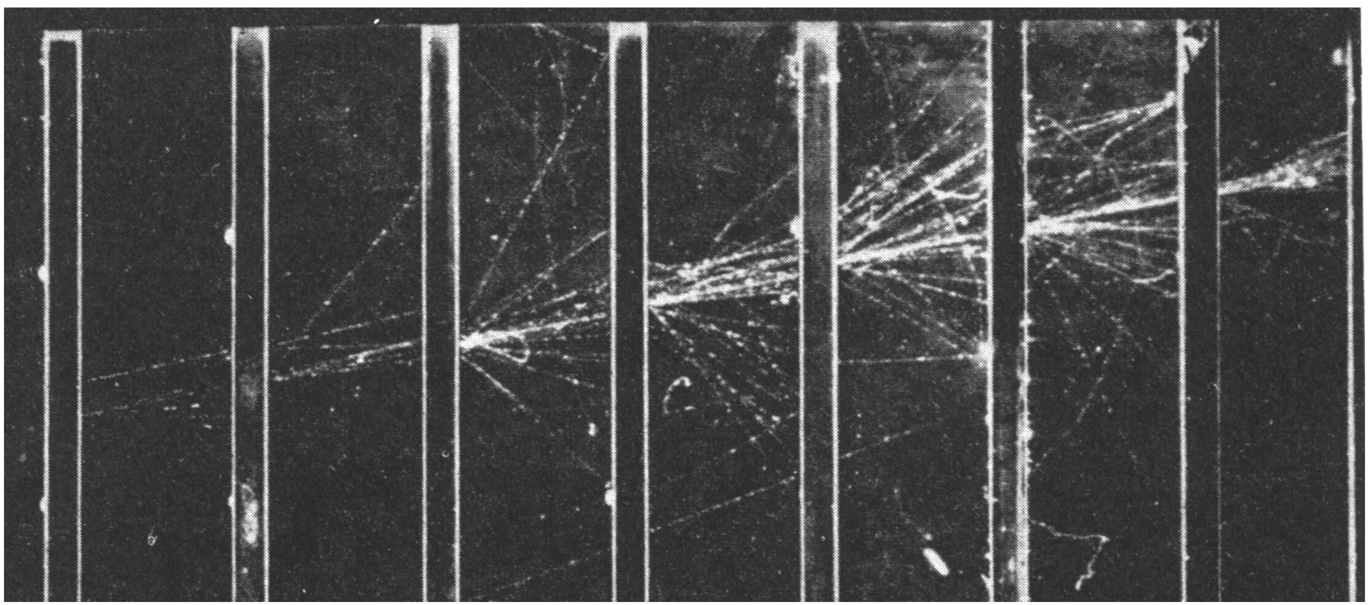

Electron shower in a cloud chamber with lead absorbers

Electromagnetic Showers

Simple Model

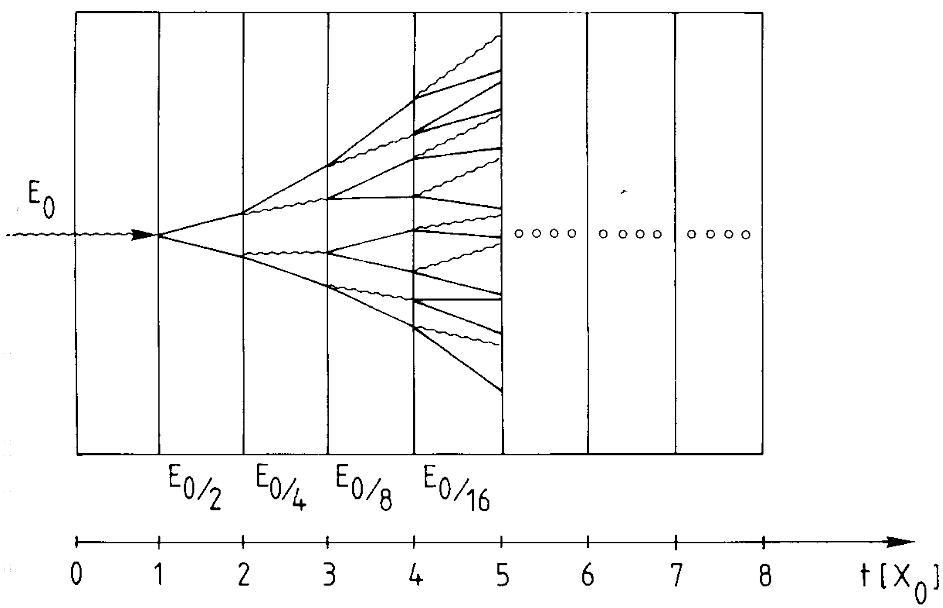

Assume only Bremsstrahlung and pairs production

After a distance t (distance in radiation length) there will be N(t) particles each with an average energy E(t):

$$N(t)=2^t \qquad E(t)/\,particle=E_0\cdot 2^{-t}$$

The process stops when $E(t)<E_c$

$$t_{\max}=\frac{\ln E_0/E_c}{\ln 2} \qquad N_{total}=\sum_{t=0}^{t_{\max}} 2^t=2^{(t_{\max}+1)}-1\approx 2\frac{E_0}{E_c}$$

For $t>t_{max}$ Compton and photoelectric effects dominate

Electromagnetic Showers

Longitudinal dimension:

$$\frac{dE}{dt} \propto t^{\alpha} e^{-t}$$

The shower maximum: $t_{\max} = \ln \frac{E_0}{E_c} \frac{1}{\ln 2}$

The 95% of the shower is in $t_{95\%} \approx t_{\max} + 0.08Z + 9.6$

Transversal dimension:

The spread of the shower is due to the multiple scattering not to the emission angles of particles. The 95% of the shower is contained within a distance of about $2R_M$:

$$R_M = \frac{21MeV}{E_c} X_0 \left[gr/cm^2\right]$$ Moliere Radius

Example: E_0 = 100 GeV in lead glass

E_c=11.8 MeV → t_{max}~13, $t_{95\%}$ ~ 23,

X_0~2 cm, R_M = 1.8·X_0~3.6 cm

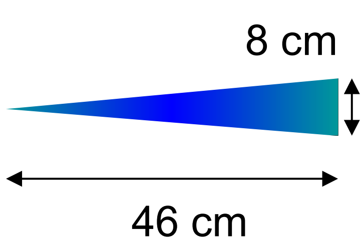

Hadronic showers

High energy hadrons interact with matter via nuclear interactions

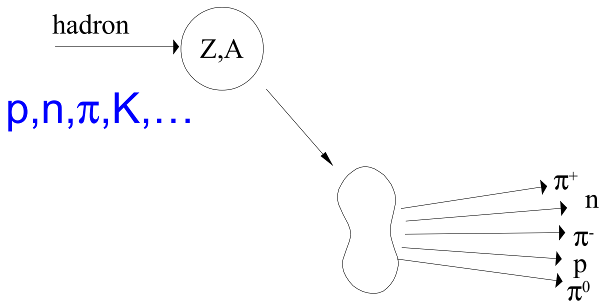

multiplicity $\propto \ln(E)$

$p_t \approx 0.35$ GeV/c

The products are:
nucleus fragments +
secondary particles

At high energy the cross section almost does not depend on the E_{in} and in analogy to X_0 we define the interaction length $\lambda_I = A/(N_A\sigma_{total}) \approx A^{1/4}$

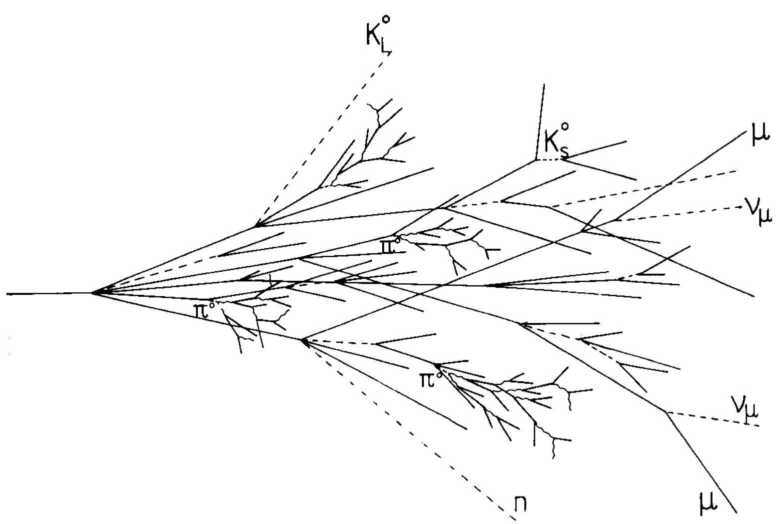

The shower has the EM and hadronic component.

The longitudinal dimension:

$$t_{max}(\lambda_I) \approx 0.2 \ln E[GeV] + 0.7$$

$$t_{95}(cm) \approx a \ln E + b$$

Iron: a = 9.4, b=39

$\lambda_a = 16.7$ cm

E =100 GeV $\rightarrow t_{95\%} \approx 80$ cm

Detectors: Fundamental Principles

Detectors used at accelerator are complex devices.

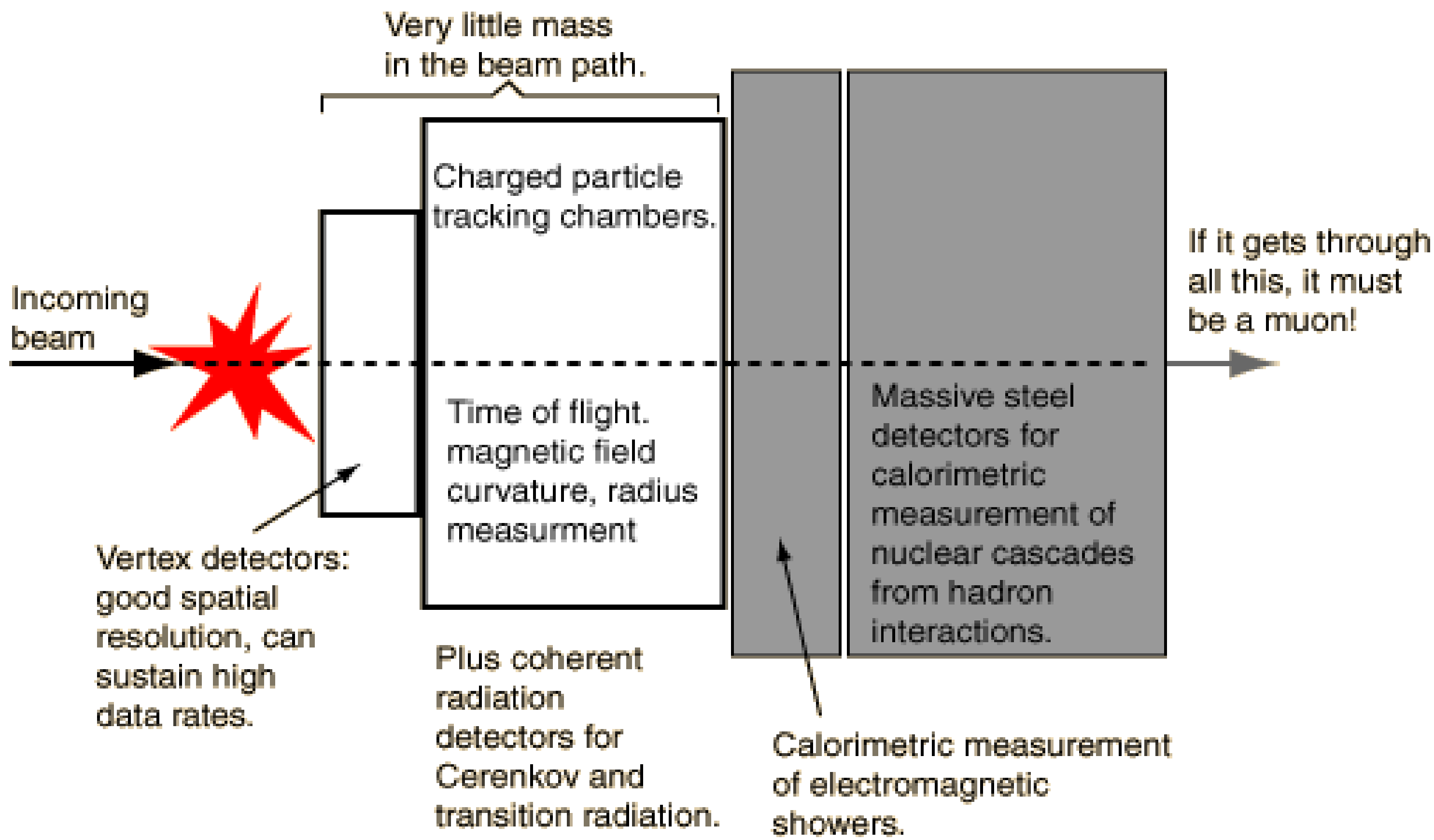

Detector for each particles

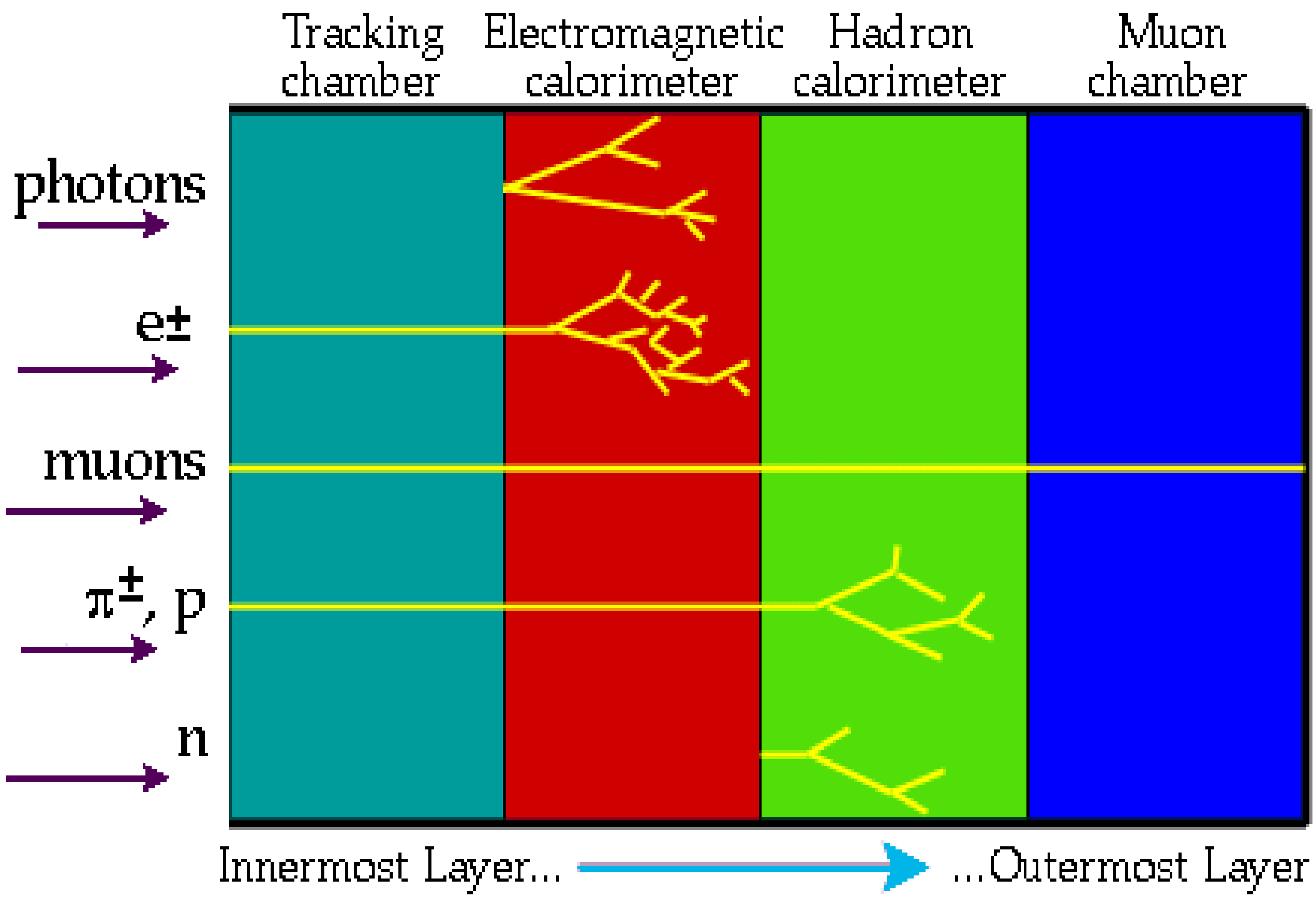

CMS Detector

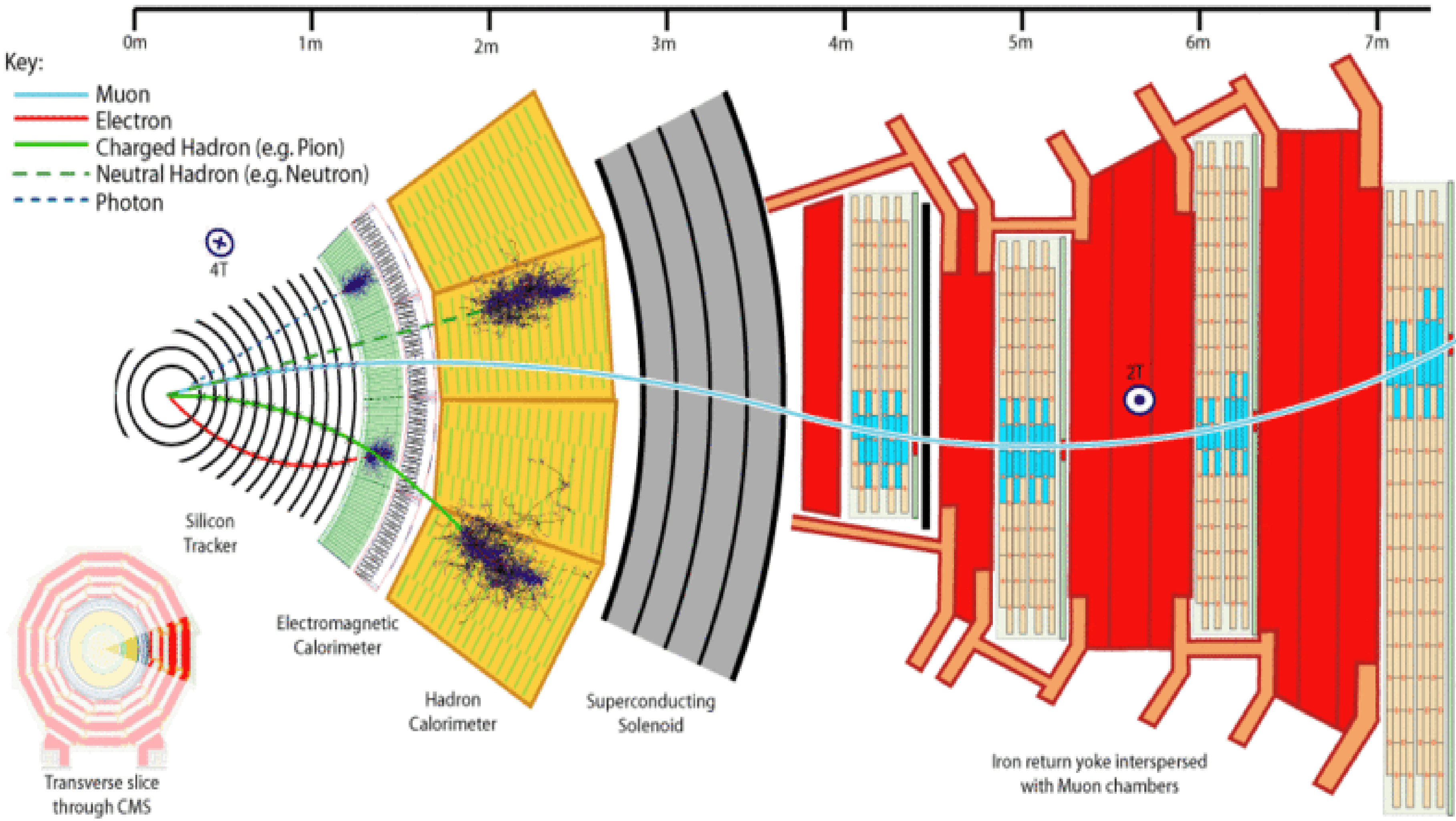

The Compact Muon Solenoid (CMS)

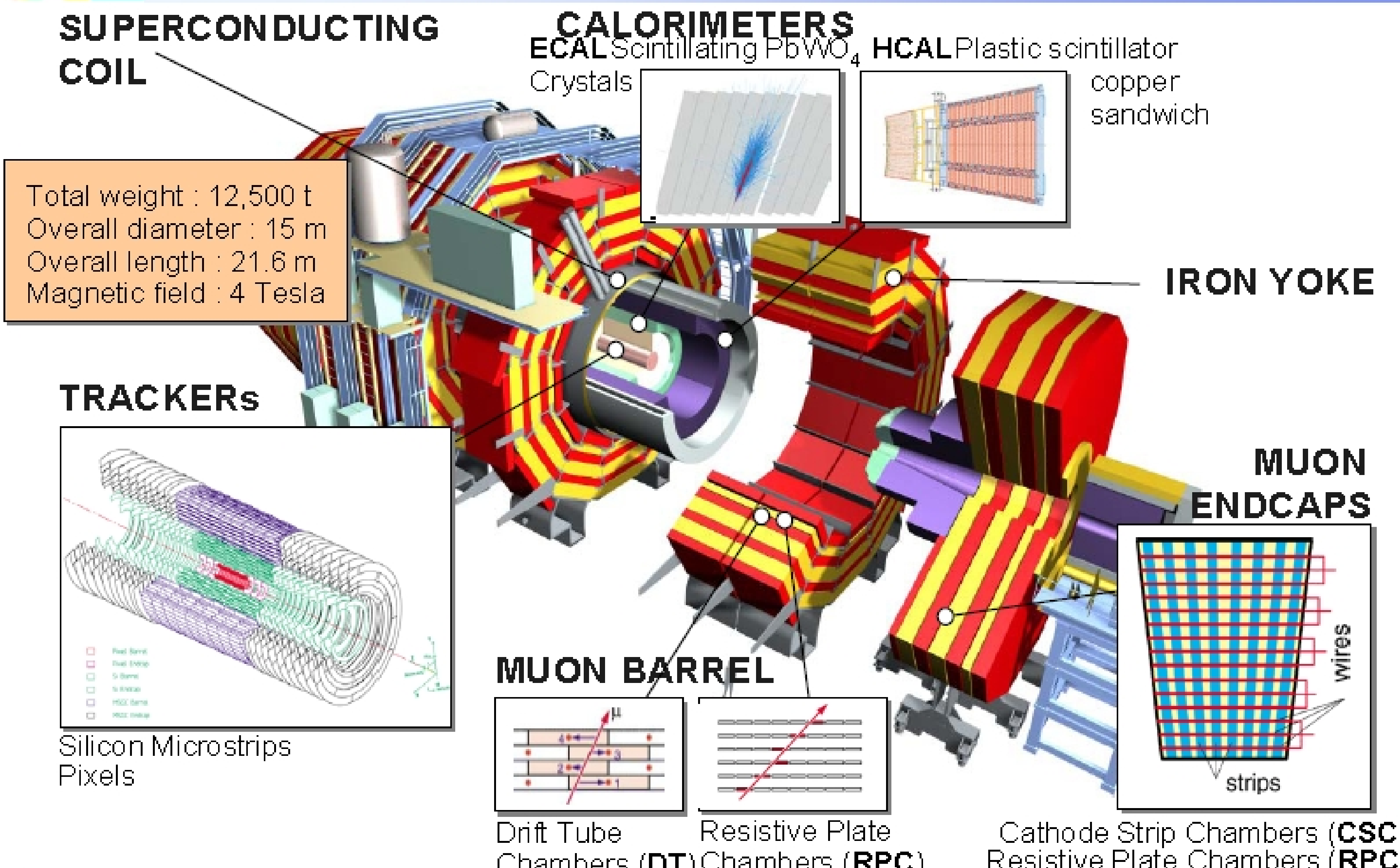

Jet Energy determination

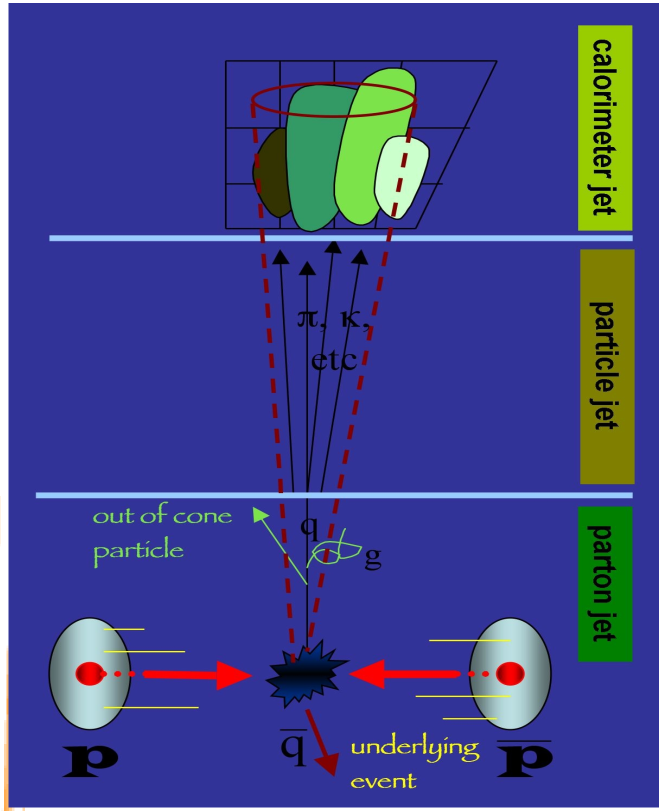

Jet energy corrections are needed to scale the measured energy of the jet back to the energy of the final state particle level jet:

- non-linearity effects and energy loss in the un-instrumented regions
- multiple interactions
- underlying event
- out of cone

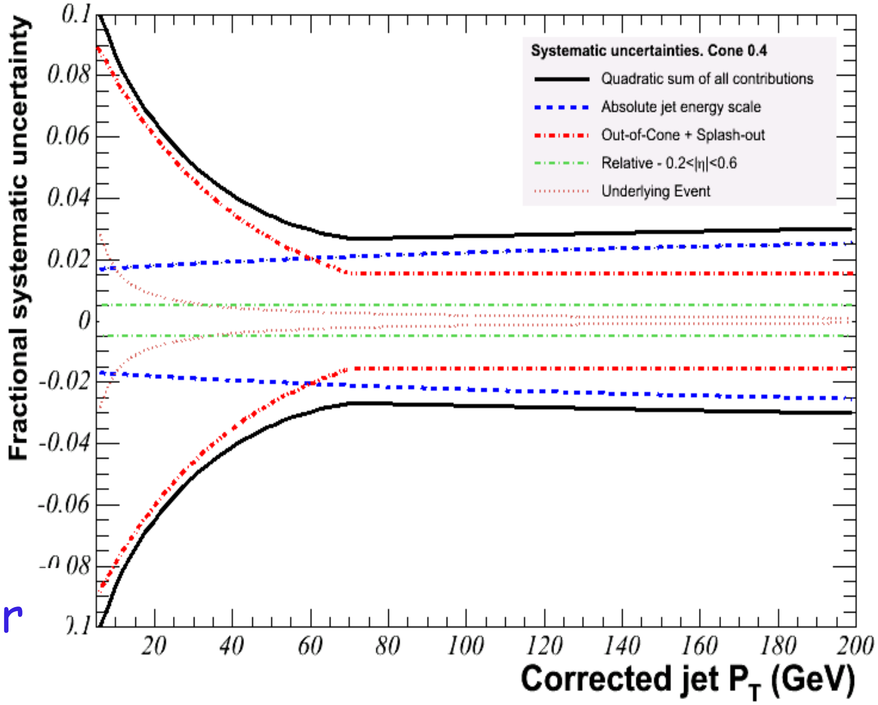

Low Pt: Dominated by MC/data uncertainties

High Pt: Dominated by calorimeter simulation uncertainties

Neutrino Identification

Not enough material in collider detectors to have neutrino interactions.

Neutrinos are identified via the transverse missing energy:

$$\vec{\not{E}}_t = \sum_{towers} E_i \sin(\theta_i)\,\hat{n}_i$$

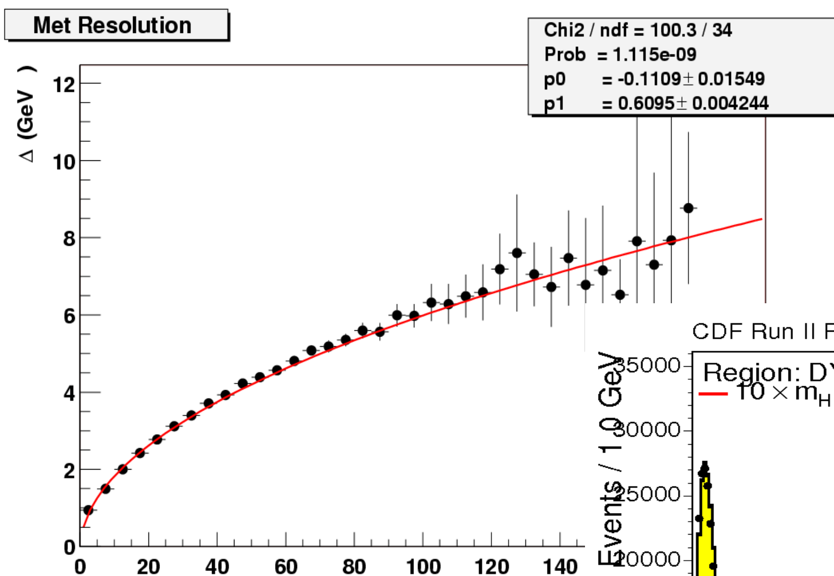

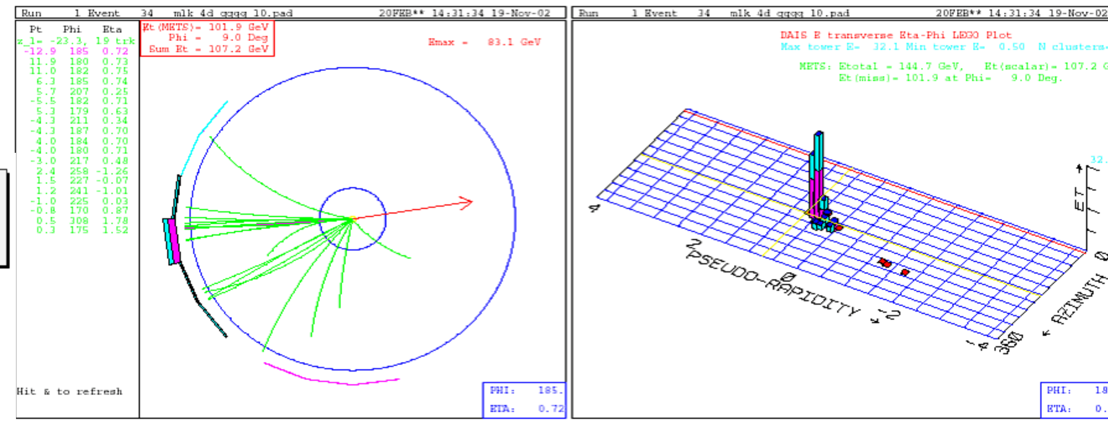

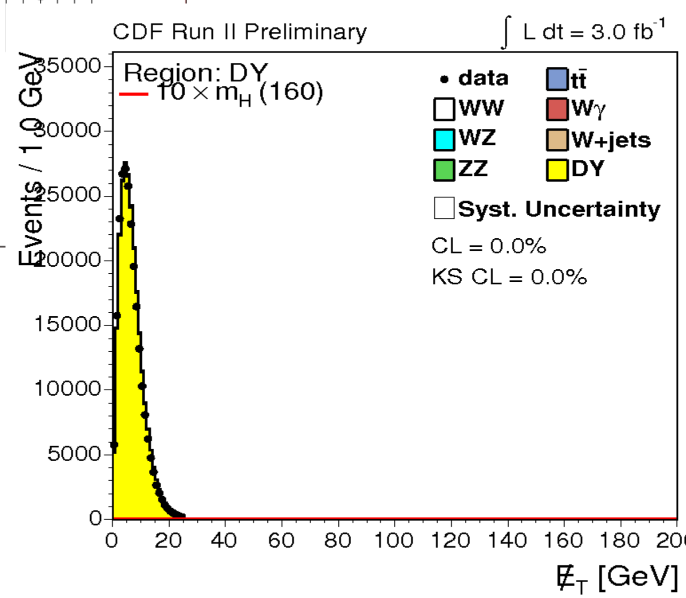

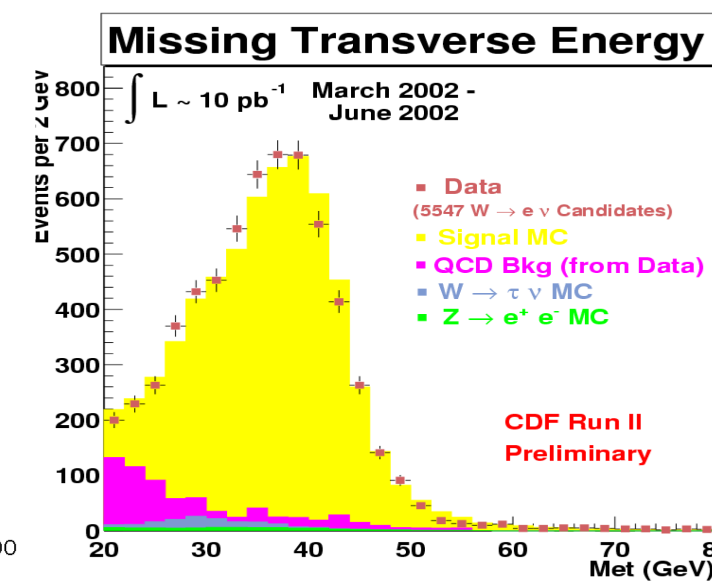

Particle Identification

TOF at CDF

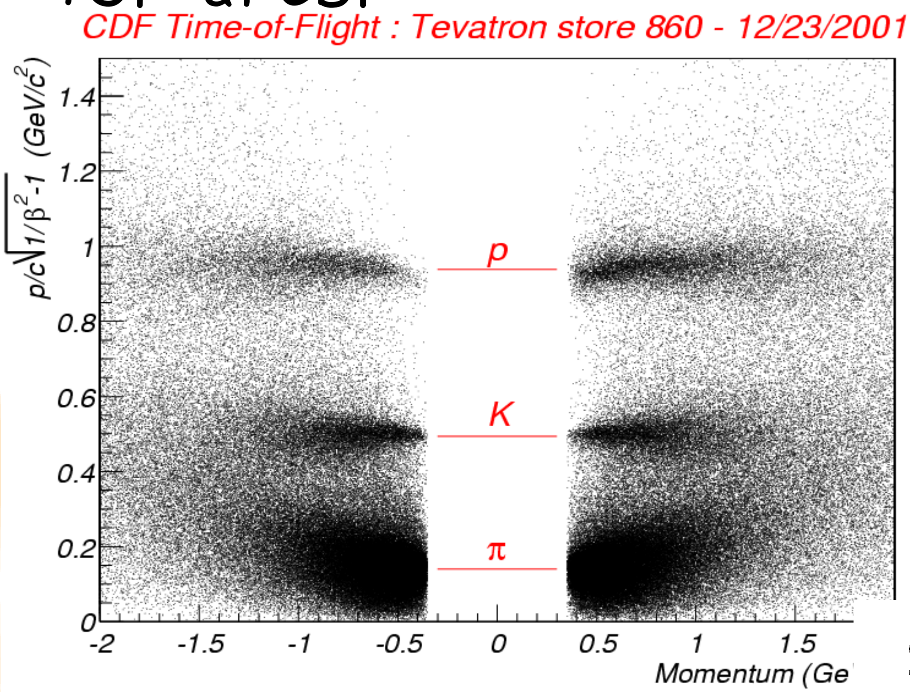

DIRC at Babar

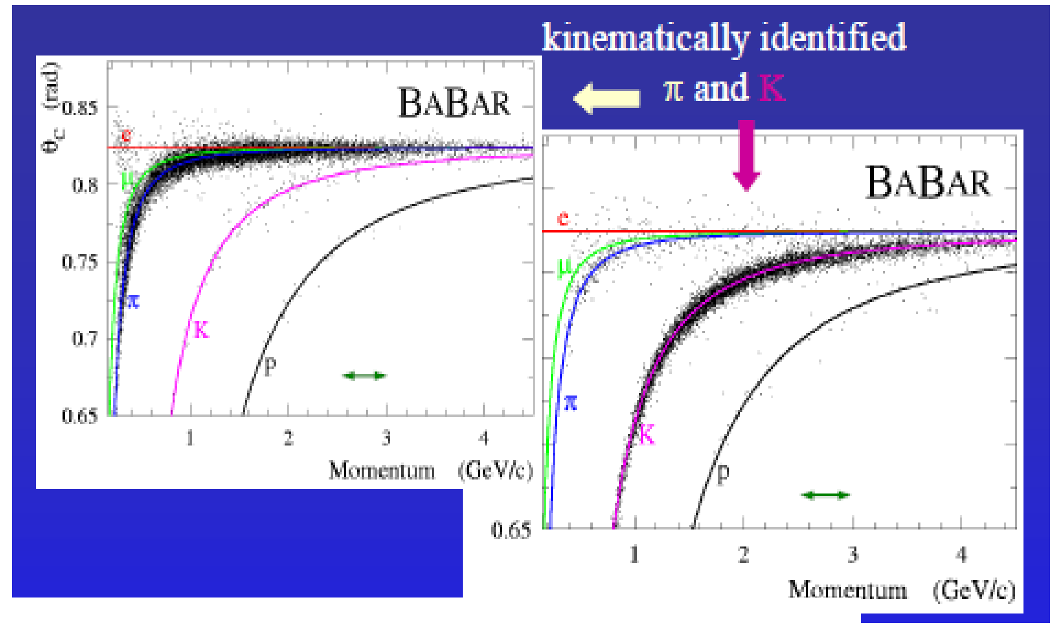

RICH at LHCb

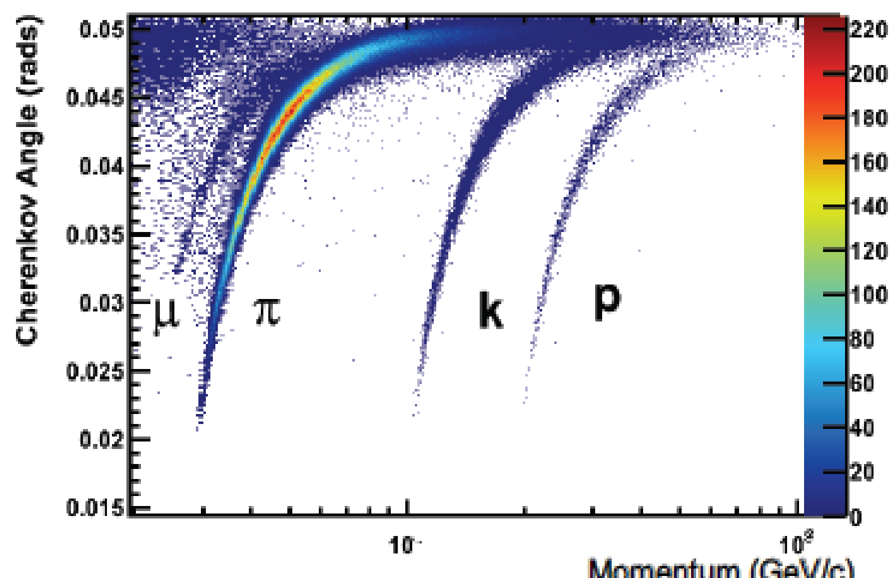

Hadron Collider: Trigger

The trigger selects events that are then written to permanent support (tape).

- The initial rate (many MHz) is reduced to few kHz.
- Usually it is structured in "levels".
- Each level must keep the selected events until the decision is taken.
- The first levels are synchronous, the system time correspond to the inter-bunch time.
- The last levels are asynchronous running non computer farm.

Hadron Collider: Trigger

Level "0": Event rate: 10^9 Hz. Detector channels: 10^7 - 10^8
DAQ is running constantly at 40 MHz. Data flow ≈ 10^{16} bit/sec

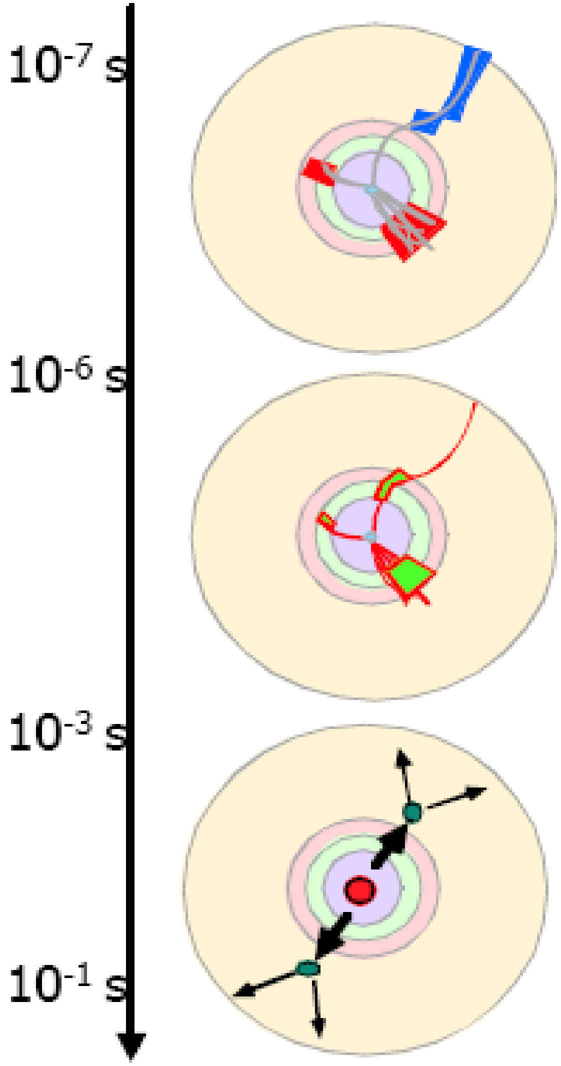

Level-1 trigger: coarse selection of interesting candidate events within a few μs. L1-rigger output rate ≈ 100 kHz
Implementation: specific hardware (ASICS, FPGA, DSP)

Level-2 trigger: refinement of selection criteria within ≈ 1 ms.
L2 output rate: ≈ 1 kHz
Implementation: fast processor farms.

Level-3 trigger: identification of the physical process. Writing data to storage medium.
L3- output rate: 10 - 100 Hz
Event size: ≈ 1 Mbyte.
Implementation: fast processor farms.

Hadron Collider: Trigger

Atlas Level 1

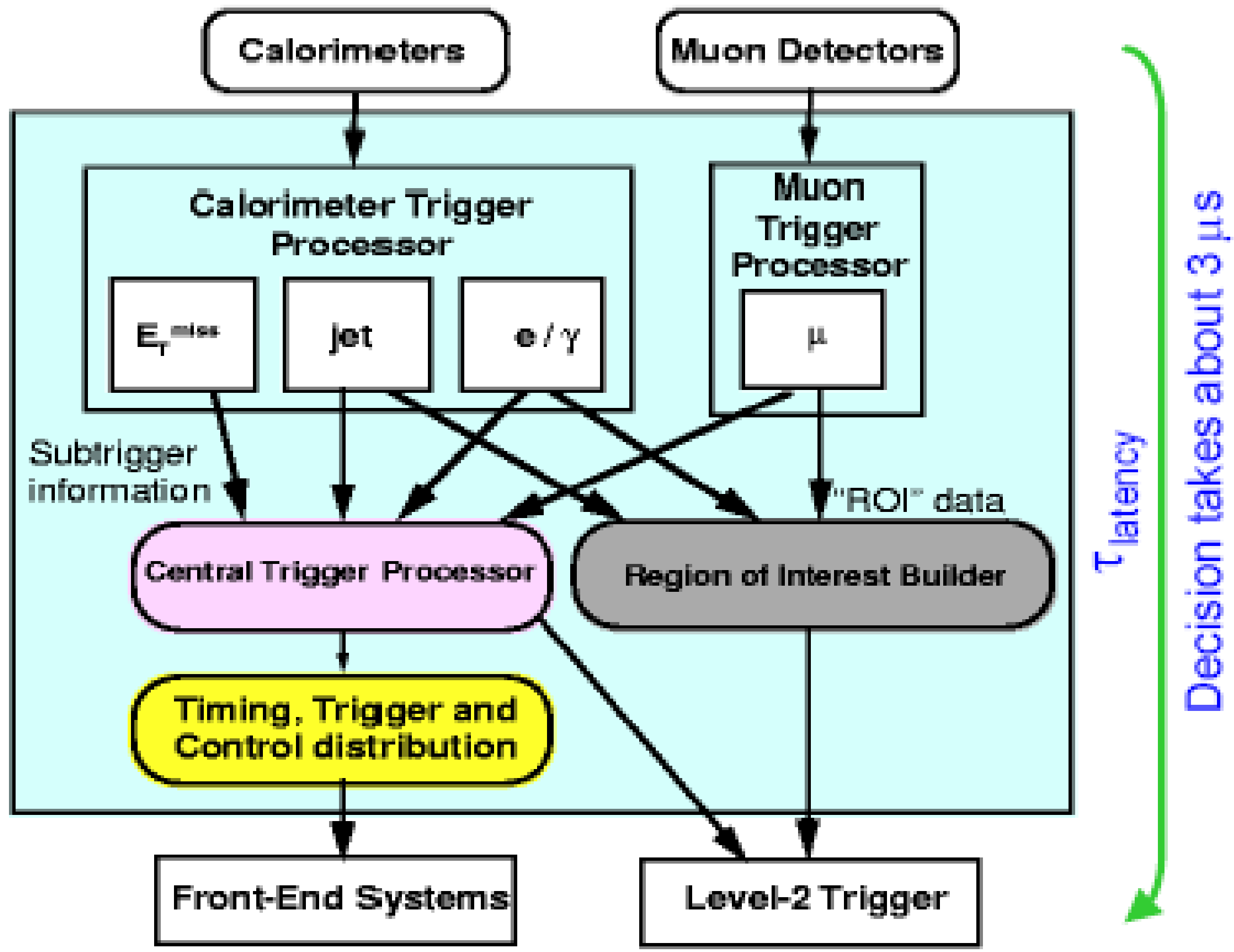

Hadron Collider: HLT τ Trigger @CMS

Regional Tracking: Look only in Jet-track matching cone
Conditional Tracking: Stop track as soon as:
If Pt<1 GeV with high C.L.

Reject event if no "leading track found" (jet is not charged)

Regional Tracking: Look only inside Isolatio
Conditional Tracking: Stop track as soon as
If Pt<1 GeV with high C.L.

Reject event as soon as additional track found (jet is not isolated)

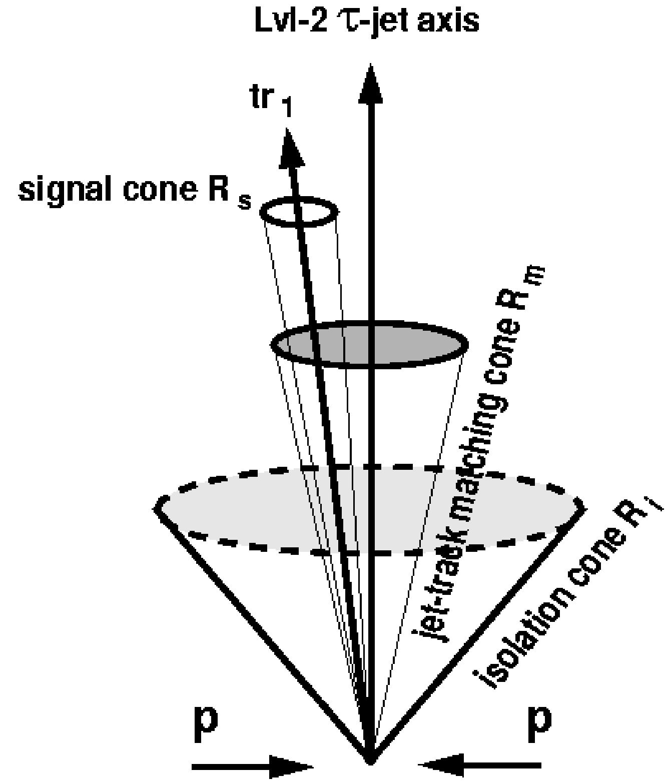

Fast enough at low luminosity for full L1 rate; at high luminosity may need a moderate Calorimeter pre-selection factor to reduce rate

Ready for the Physics!